

Review

Molecular Logic Gates Based on Ferrocene-Containing Compounds

Christina Eleftheria Tzeliou ^{1,2} , Konstantinos P. Zois ^{1,3}  and Demeter Tzeli ^{1,2,*} 

¹ Laboratory of Physical Chemistry, Department of Chemistry, National and Kapodistrian University of Athens, Panepistimiopolis Zografou, 157 84 Athens, Greece; ctzeliou@chem.uoa.gr (C.E.T.); kpzois@chem.uoa.gr (K.P.Z.)

² Theoretical and Physical Chemistry Institute, National Hellenic Research Foundation, 48 Vassileos Constantinou Ave., 116 35 Athens, Greece

³ Inorganic Chemistry Laboratory, National and Kapodistrian University of Athens, Panepistimiopolis Zografou, 157 71 Athens, Greece

* Correspondence: tzeli@chem.uoa.gr; Tel.: +30-210-727-4307

Abstract: Ferrocene has a unique structure, i.e., a central iron atom neatly sandwiched between two cyclopentadienyl rings, which has revolutionized the chemists' views about how metals bind to organic π -systems. This structural arrangement leads to some fascinating chemical and photophysical properties. The last three decades, there were reports about receptor molecules that could be considered to perform simple logic operations via coupling ionic bonding or more complex molecular-recognition processes with photonic (fluorescence) signals. In these systems, chemical binding ('input') results in a change in fluorescence intensity ('output') from the receptor. It has been proven that molecules respond to changes in their environment, such as the presence of various ions, neutral species, pHs, temperatures, and viscosities. Since their first realization by de Silva, molecular logic gates have been intensively experimentally studied, with purely theoretical studies being less common. Here, we present the research that has been conducted on Molecular Logic Gates (MLGs) containing ferrocene and their applications. We categorized such systems into three families of MLGs: long-chain molecules (oligomers or polymers) that incorporate ferrocene, medium-sized molecules that incorporate ferrocene, and systems where ferrocene or its derivatives are used as external additives. Furthermore, MLGs including metal cations without the ferrocene moiety are briefly presented, while computational methodologies for an accurate theoretical study of MLG, including metal cations, are suggested. Finally, future perspectives of MLGs containing ferrocene and their applications are also presented.

Keywords: ferrocene; molecular logic gates; Fe; transition metal cation; sensors; organometallic compounds



Citation: Tzeliou, C.E.; Zois, K.P.; Tzeli, D. Molecular Logic Gates Based on Ferrocene-Containing Compounds. *Inorganics* **2024**, *12*, 106. <https://doi.org/10.3390/inorganics12040106>

Academic Editors: Mojca Čakić Semenčić and Lidija Barišić

Received: 29 February 2024

Revised: 1 April 2024

Accepted: 3 April 2024

Published: 6 April 2024



Copyright: © 2024 by the authors. Licensee MDPI, Basel, Switzerland. This article is an open access article distributed under the terms and conditions of the Creative Commons Attribution (CC BY) license (<https://creativecommons.org/licenses/by/4.0/>).

1. Introduction

Logic Gates: Logic gates are devices used to perform binary arithmetic and logical operations and thus constitute the basis of modern computers. They perform Boolean logic operations on one or more inputs to produce an output. Each type of logic gate possesses a specific input–output signal correlation pattern described in the so-called truth table, which lists all the possible combinations of input–output states. Generally, molecular switches convert input stimulations into output signals. Therefore, the principles of binary logic can be applied to the signal transduction operated by molecular switches. It is not necessary for the inputs and outputs to share the same logic convention; thus, different conventions applied to the same molecular device can lead to different logic functions. The most common logic operators are YES, NOT, AND, OR, NOR, NAND, INHIBIT, and XOR, and they process the truth or falsity of one or two statements in characteristic ways [1–3].

Molecular Logic Gates: Before the landmark publication by de Silva et al. in 1993 [4], there were already reports [5–8] about receptor molecules that could be considered to

perform simple logic operations by coupling ionic bonding or more complex molecular-recognition processes with photonic (fluorescence) signals. In these systems, chemical binding (the 'input') results in a change in fluorescence intensity (the 'output') from the receptor.

Photo-induced electron transfer has become established as an important principle in photochemistry. In 1985, de Silva et al. showed how this principle could be profitably applied to solve several problems concerning fluorescent pH indicators. Most are phenols, anilines, or heterocyclic derivatives where the acid-base site is an integral part of the chromophore. The aminomethyl-anthracene derivatives under study formed fluorescent pH indicators with spectral properties independent of substituents and pH except for the fluorescent quantum yield, showing that their pK_a^* values are identical to the corresponding pK_a values [5].

In 1988, Aviram theoretically studied the potential use of a conjugated molecule of at least 50 Å long as a pro-conductor or a conductor when placed between two metallic electrodes with the long axis of the molecule perpendicular to the metal surfaces. The spiro bridge proposed in this work was rather unique, as it could localize an electron on one side of a molecule by providing a large tunneling barrier. The same bridge was also flexible toward electron transfer in electric fields, above the threshold. Additionally, the exchange of the conductivity properties of the terminal groups did not go unnoticed, leading to possible device application in areas of signal processing at the molecular level. The results of the dipole switching due to the action of the field above the threshold and the simultaneous collapse of the tunneling barrier were found to be complementary to each other. Calculations that were performed indicated that the proposed model has the device properties that were presented and Aviram felt that the model could serve as a blueprint for molecular electronics [9].

In 1993, de Silva et al. opted for an anthracene derivative as the receptor of the molecular logic gate they synthesized. Anthracene derivatives had previously been shown to undergo Photoinduced Electron Transfer (PET) processes via the separate actions of tertiary amines and benzocrown ethers. These transfer processes could be suppressed by the injection of protons and sodium ions, respectively, to cause the 'switching on' of fluorescence. This molecule was based on the 'fluorophore-spacer1-receptor1-spacer2-receptor2' format. Therefore, the fluorescence of the molecule would occur only when the tertiary amine and the benzocrown ether units received proton and sodium ion input, respectively. This molecule successfully operated as a two-input AND logic gate, as tertiary amines and benzocrown ethers are highly selective for protons and sodium ions, respectively. Thus, each receptor will accept its designated ion independently and both receptors are independently capable of quenching the emission via excited state electron transfer. This means that the molecule in the solution behaves as an AND logic gate, with H^+ and Na^+ being "inputs" and the emission intensity serving as the output. Consequently, the molecule can self-select its input ionic signals into the appropriate site as soon as it is provided with high enough concentrations of protons and sodium ions, which are chosen by the operator. The fluorescence signals from single molecules can be received and analyzed by spectroscopy [4].

It has been proved that molecules respond to changes in their environment. The presence of various ions, neutral species, pHs, temperatures, and viscosities, among other factors, result in color or emission changes because of the complex interplay of many excited state processes and environmental parameters [10].

Ferrocene: Ferrocene (Fc) was synthesized in 1951 by Kealy and Pauson [11], while its structure was revealed in 1952 by Wilkinson et al. [12]. Ferrocene has a unique structure, i.e., a central iron atom neatly sandwiched between two cyclopentadienyl rings, which has revolutionized the chemists' views about how metals bind to organic π -systems (Figure 1). This structural arrangement leads to some fascinating chemical and photophysical properties. Its electronic structure and ultraviolet-visible (UV-visible) light absorption spectra have been extensively analyzed [13–15]. Pure ferrocene is a very stable light orange powder, while, upon cooling, the color changes from orange to lemon yellow [13]. The orange

color results from a forbidden dipole absorption at 440 nm and a shoulder at 528 nm. The strongest absorption peak is observed at 202 nm in solution and 196 nm in the gas phase. The oscillator strength of the allowed absorption is 350 times stronger than that of the peak at 440 nm [13–16].

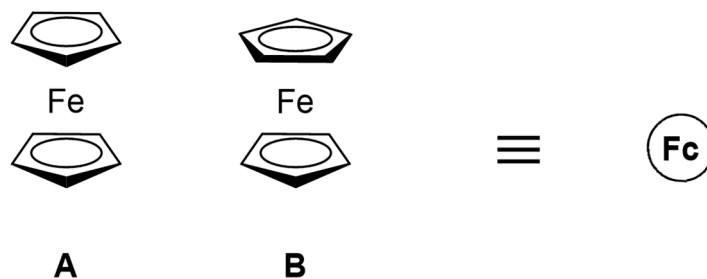


Figure 1. The two possible conformations of ferrocene: eclipsed (A) and staggered (B). Henceforth, ferrocene and “Fc” will be used interchangeably and the ferrocene moiety in compounds mentioned herein will be denoted as a circled Fc.

Ferrocene can easily donate an electron in a molecular system designed according to the principles of modular photoelectron transfer, i.e., in the ‘fluorophore–spacer–receptor’ or ‘fluorophore–spacer–receptor1–spacer–receptor2’ format via redox chemistry. Thus, ferrocene derivatives have potential applications as MLG systems [17–20].

In the present review, novel synthesized and/or calculated ferrocene-based molecular logic gates are described in Section 2, in which their structural, photochemical, and electrochemical characteristics are analyzed. In Section 3, MLGs including metal cations without the ferrocene moiety are briefly presented. In Section 4, computational methodologies for an accurate theoretical study of MLGs including metal cations are suggested. Finally, in Section 5, the conclusions and future perspectives are discussed.

2. Work on Ferrocene-Based MLGs

Since their first realization by de Silva, logic gates have been intensively experimentally studied at the molecular level, with purely theoretical studies being less common and such work mainly being carried out to complement the experimental findings. The same applies to MLGs that incorporate the ferrocene moiety in one way or another. Experimental studies of such systems can be roughly categorized into three distinct families of MLGs: (1) long-chain molecules (oligomers or polymers) that incorporate ferrocene, (2) medium-sized molecules that incorporate ferrocene, and (3) systems where ferrocene or its derivatives are used as external additives. These three families are elaborated below.

2.1. Long-Chain Molecules as Logic Gates (LC-MLG)

This first family of MLGs includes oligomeric molecules that form self-assembled monolayers (SAMs) or polymeric materials that integrate a ferrocene moiety. In the latter case, a medium-sized MLG, see below, is synthesized in such a way that it can be subsequently attached to a polymer chain; otherwise, the ferrocene moiety belongs a priori to the polymer chain as part of the monomer being used. In both cases, it is apparent that such MLG systems are easily scalable and transformable to a device. The bibliography is not as rich in comparison to the second family (see below), presumably due to the more delicate chemical handling required for such systems, which is, of course, not possible for the optoelectronics and physics communities, which are usually studying such systems. Thus, quite straightforwardly, a rich field of prosperous collaborations between different scientific communities appears.

A recent and informative example of such an LC-MLG featuring SAMs is that of Li, Nijhuis, del Barco et al. [20], who reported a prototype single-electron logic calculator (SELC) based on the oligomer Au-S-(CH₂)₃-Fc-(CH₂)₉-S-Au. This was used as a bridge between two gold nanoelectrodes, ultimately tuning the way electrons are transferred. Its

operating principle is based on predictable and reliable current conversions modulated by voltages crossing the stable Coulomb blockade regime, avoiding dependence on an absolute current and improving function reproducibility. Compared to other approaches, the non-conjugated asymmetric Fc-based molecule naturally provides logic operations via its robust and unique Coulomb blockade characteristics. The authors managed to exploit the system's properties and bring out all possible 1- and 2-input logic operations (YES, NOT, PASS_1, PASS_0 and AND, XOR, OR, NAND, NOR, INT, XNOR) through a fine interplay between gate voltage and bias voltage, which were the two inputs. For the two-input logic gates, phase control between the two voltages was the key.

Polymeric materials featuring ferrocene are closer to the chemist's mindset and have been an area of study, due to their logical behavior, for quite some time. One of the first such studies was that of Matsui, Miyashita, and coworkers [21], who used assemblies based on polymeric nanosheets that contain ferrocene and $[\text{Ru}(\text{bipy})_3]^{2+}$ in their monomeric units. The chemical structure of the polymers is represented below (Figure 2A). Cathodic and anodic photodiodes based on these polymers were the heart of the device and, overall, the devices could be used as OR and XOR MLG. Excitation light from either side of the device was used as the two-input scheme and the measured photocurrent was the system's output.

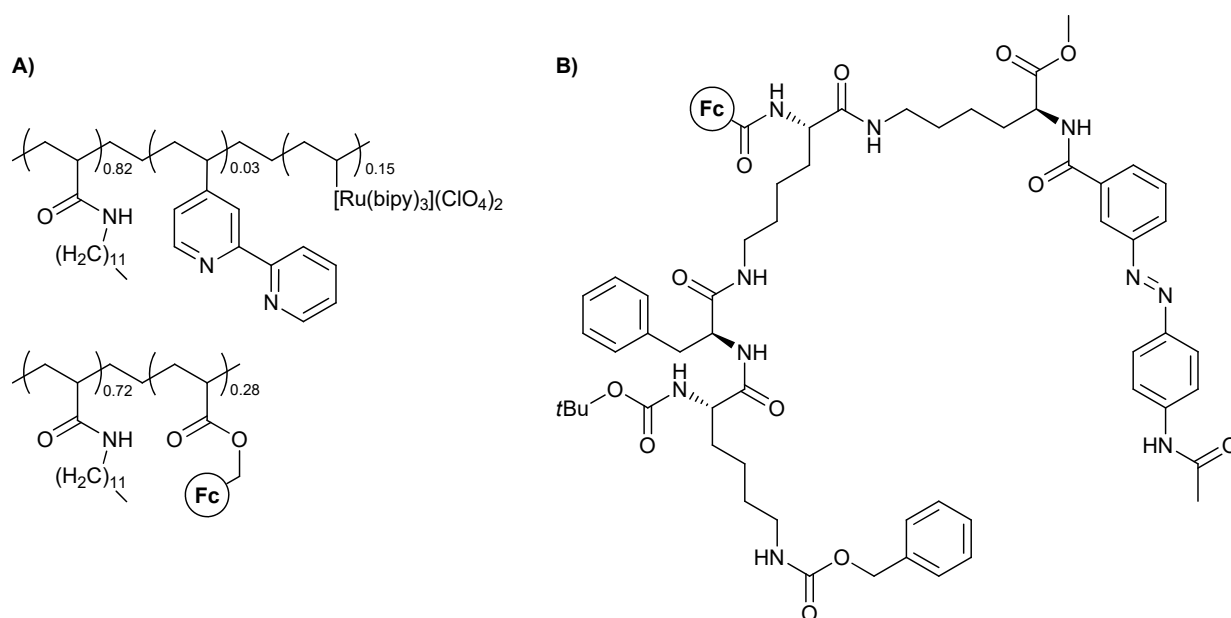


Figure 2. Molecular structures for (A) the organometallic polymers used as polymer nanosheet photodiodes and (B) the metallogelator featuring the gelation transition as the output of the logic function.

Another interesting example is that of a metallogelator yielding a logic gate operation, reported by Afrasiabi et al. in 2012 [22]. The molecule undergoes a gel formation procedure in acetone upon sonication and exhibits responsiveness to external signal-inputs. The molecular structure of it is presented below (Figure 2B), while two simpler analogues were used by the authors to further investigate the validity of their claims. NOT and XOR logic operations could be realized depending on the redox conditions used.

In 2019, Magri et al. [23] demonstrated a family of naphthalimide-based fluorescent logic gates, represented by PASS 0, PASS 1, YES (H^+ TRANSFER), and AND logic functions, in solution at the molecular level and covalently bound onto TentaGel polymer beads at the micrometer level. Ferrocene acts as the electron donor in the molecules that were designed according to the 'electron-donor-spacer1-fluorophore-spacer2-receptor-linker-bead' format. The ground and excited state electronic structures were computed via Density Functional Theory (DFT) methodology using Unrestricted Hartree-Fock (UHF), DFT, and

TD-DFT methods, i.e., UHF/TZVPP2 and DFT(B3LYP)/TZVPP2, in good agreement with the corresponding experimental data.

Following this, Magri et al. [24] synthesized a medium-sized molecule based on previously developed design principles (see the MS-MLG family), which can be readily attached to a polymeric bead (Figure 3). The final logic system exhibits the INHIBIT logic function, with enhanced fluorescence serving as an output only when oxidant levels are high and proton levels remain low. The non-polar environment of the polymer beads was said to contribute further to the output enhancement.

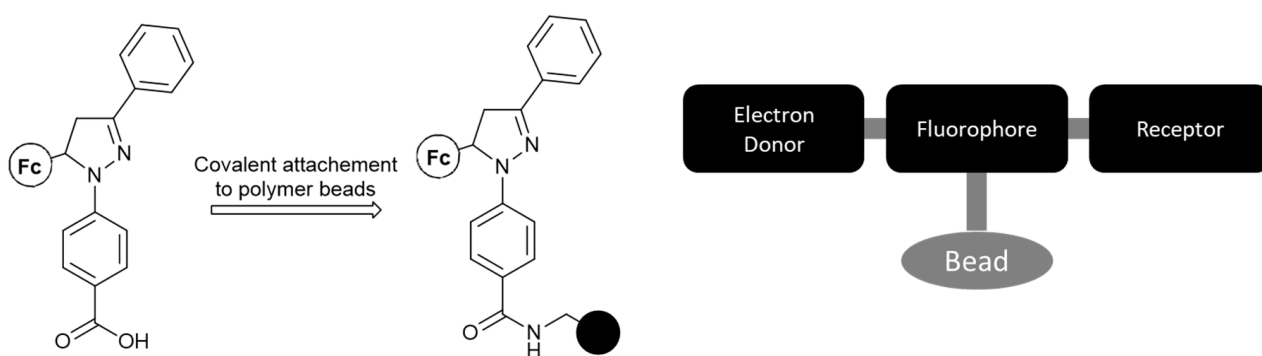


Figure 3. The synthesized molecule features a carboxylic end-functionality, which can be readily coupled with the amine pendant-group of a polymeric bead (black circle). The system features the following format: electron-donor–spacer–fluorophore–spacer–receptor, which has been shown to yield desirable and manageable results with respect to logic gate functionality.

Overall, this field of long-chain molecules that are able to perform logic operations seems to be underdeveloped, with few examples (see also References [25–29]). Nevertheless, the possibility of synthesizing such macromolecules with tailor-made characteristics appears quite attractive. Such systems occupy the whole breadth of logic operations, and thus it seems worthwhile to work on this area. Furthermore, systems such as that of Ref. [20] may be the most prominent concerning their applicability, as they can be tuned to every logic gate virtually with only minor changes.

2.2. Medium-Sized Molecules as Logic Gates (MS-MLG)

The second family of ferrocene-based MLG presented in this work seems to be the most studied compared to the other two. As such, this family will be broken up into parts that are approximately based on the fluorophore of the molecule. This categorization seems to be the most appropriate since the fluorophores of such molecules have not seen much “experimentation”. Anthracene and naphthalimide are two well-studied fluorophores, and thus will represent two categories by themselves. A third category will be that of other fused heterocycles, and finally a fourth category will encompass molecules that do not fit to the previous three. Moreover, such studies involving medium-sized molecules allow for the computational description of the system based on useful theoretical models such as DFT, and thus a handful of such reports combine theory and experiment.

I. Fc-based MS-MLG containing anthracene as fluorophore.

The use of the anthracene moiety as a fluorophore has long been realized in the realm of ferrocene-based MLGs, although its implementation has not been that successful compared to naphthalimide. This can be rationalized based on the synthetic difficulties of molecules based on anthracene and the comparatively bad tunability of anthracene’s optical and redox properties. Nevertheless, such compounds were important for the development of the field and useful design guidelines were created for the improvement of these sensors.

The first example of anthracene-containing MS-MLG and one of the first works of ferrocene-based MLG is presented in the report by Fang, Yan et al., in 2008 [30] (Figure 4). The authors exploited ferrocene’s great redox characteristics to control the PET process,

along with its solubility and cost-effectiveness. An AND logic gate could be realized using acidic and oxidizing conditions as inputs and the fluorescence of the molecule as an output. Only when both inputs are high does the molecule surpass the PET-quenching effect of ferrocene and emit at 438 nm with a three-fold enhancement.

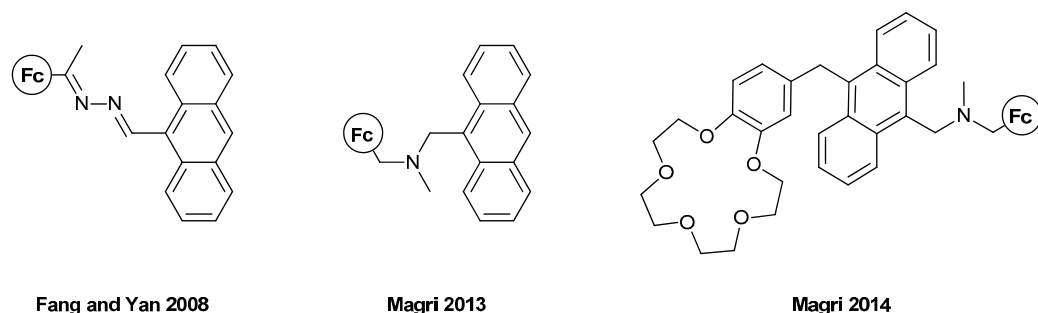


Figure 4. Three ferrocene-based molecular logic gates based on the fluorescence properties of anthracene, Refs. [30–32].

Two other examples in 2013 [31] and 2014 [32] from the team of Magri are rather informative (Figure 4). In 2013, they synthesized an AND MLG with a similar molecular engineering as presented above: electron donor–proton receptor–fluorophore. Again, only when both proton and oxidizing concentrations were high was the fluorescence output also high. A remarkable fivefold increase in the fluorescence intensity of around 400 nm was reported, which is also observable with the human eye. The same group, in 2014, reported another AND MLG, which featured the “lab-on-a-molecule” approach reported previously by de Silva. Using this molecule, a three-input MLG can be constructed (Na^+ , H^+ and Fe^{3+}) where the output is again the fluorescence from the anthracene moiety. The three-fold fluorescence enhancement can be exploited in numerous circumstances where MLGs with more than two inputs are necessary, such as corrosion detection and tumor cell diagnosis. The fluorescence peaks were again ca. 400 nm.

II. Fc-based MS-MLG containing naphthalimide as fluorophore.

The majority of work on the MS-MLG family includes the use of naphthalimide (NA) as the fluorophore of the MLG, mostly because of the available synthetic procedures involving this moiety and the desirable tunability of its redox/fluorescence properties. Due to the symmetry degeneration induced by its structure, NA-based MLGs appear in different fashions, as shown below (Figure 5). These modular structures result in a plethora of tunable characteristics for the obtained MLG, as can be seen in the following discussion.

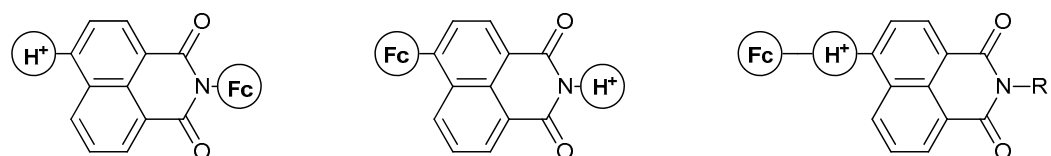


Figure 5. Different molecular designs of the naphthalimide-containing Molecular Logic Gates. “Fc” resembles the position of the ferrocene moiety, while “H⁺” resembles the position of the proton receptor.

Zhu et al. reported, in 2012 [33], one of the first examples of a molecule that contains both the NA and Fc moieties that is able to show “logic”. Although not involving molecular logic gate studies, this work showed the successful combination of NA and Fc, where oxidation of the Fc moiety can result in PET quenching and therefore yield the ON-OFF (1-0) states of fluorescence. Irradiation with a specific wavelength could induce photocyclization of the bisthiénylene. Overall, gated photochromism could be realized, and five different states could be achieved from a single molecular platform (Figure 6).

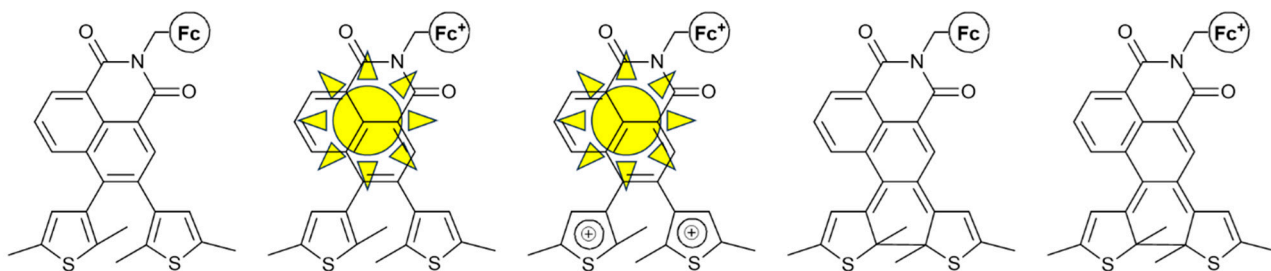


Figure 6. The five different states of the same molecular structure reported in [33]. Only the second and third states are able to fluoresce.

In 2015, Zhu, Marken, and James et al. [34] used this efficient combination of NA and Fc to synthesize molecule **1**, as shown in Figure 7. The way the NA and Fc moieties are attached is the same, but in this case the molecule contains a boronic acid site, which is able to sense F^- ions and stick to polymeric substrates. The piperazine group has not been studied for its potential proton-sensing properties, but rather acted as a linkage. The studies involved the molecule as a multi-input logic gate, with the inputs being the Fe^{3+} and F^- ions and sodium L-ascorbate (LAS), the latter acting as a reducing agent. As a two-input MLG, the authors used Fe^{3+} and LAS or F^- , yielding an INHIBIT logic gate. Using all three inputs, a combinational NOR and AND logic circuit could be realized.

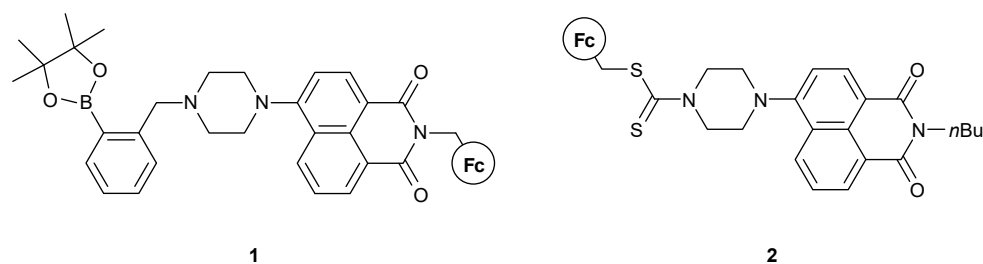


Figure 7. Molecular structures of the sensors of Refs. [34,35].

Zhang et al. [35] reported **2** (Figure 7), which could provide human-eye detection of Cu^{2+} and Hg^{2+} ions. They showed that the detection process is not pH-dependent and can readily be used in aqueous solutions. The ion interaction of compound **2** and the two analytes is selective in the presence of other competitive cations used in the study. The molecule acted as a binding site for Hg^{2+} , while Cu^{2+} induced PET-quenching through the oxidation of the Fc moiety. Although explicit logic gate experiments have not been conducted, its ability to act as an MLG is apparent.

During the last decade, Magri's group has made considerable progress towards the realization of efficient MLGs containing ferrocene as the redox probe of the system. Using the NA moiety as the fluorophore is common practice in their work and they have managed to successfully introduce many logic processes using this molecular design. The assembly of an MS-MLG incorporating both NA and Fc is shown in Figure 8. As can be seen, all the different ways (Figure 5) that the Fc group can be introduced relative to the NA moiety are realized. Thus, a plethora of results are obtained for the logic operations.

Clearly, structures **3** [36], **7** [17] and **8** [17] can be readily compared due to their structural similarities, i.e., the Fc group is attached through a methylene-linker to the N-atom of the NA backbone, while the proton acceptor group resides on the other side; see Figure 8. As before, the fundamental molecular engineering is based on the PET quenching process, resulting from the oxidation of the Fc moiety. The additional part is the way the proton receptor behaves upon protonation and the implications for fluorescence due to this potential change. In the case of **3**, protonation leads to a twisted conformation of the piperazine group, yielding a non-emissive, excited Internal Charge Transfer (ICT) state. Thus, a 13-fold emission enhancement is realized only when protonation and oxidation

occur simultaneously, leading to an AND logic gate. Similarly, compounds **7** and **8** also present examples of AND MLG, featuring a 16-fold and 10-fold fluorescent enhancement, respectively. The report for these two compounds included time-resolved fluorescence spectroscopy, along with DFT calculations, which both corroborated with an advantageous driving force of charge transfer assisted by a positive electric field at the four-amino end of the fluorophore, featured in all three compounds. Compound **8** was designed with an ‘electron-donor-spacer1-fluorophore-spacer2-receptor’ format. All theoretical calculations were carried out employing the UHF and DFT(B3LYP)/TZVPP2 methodology.

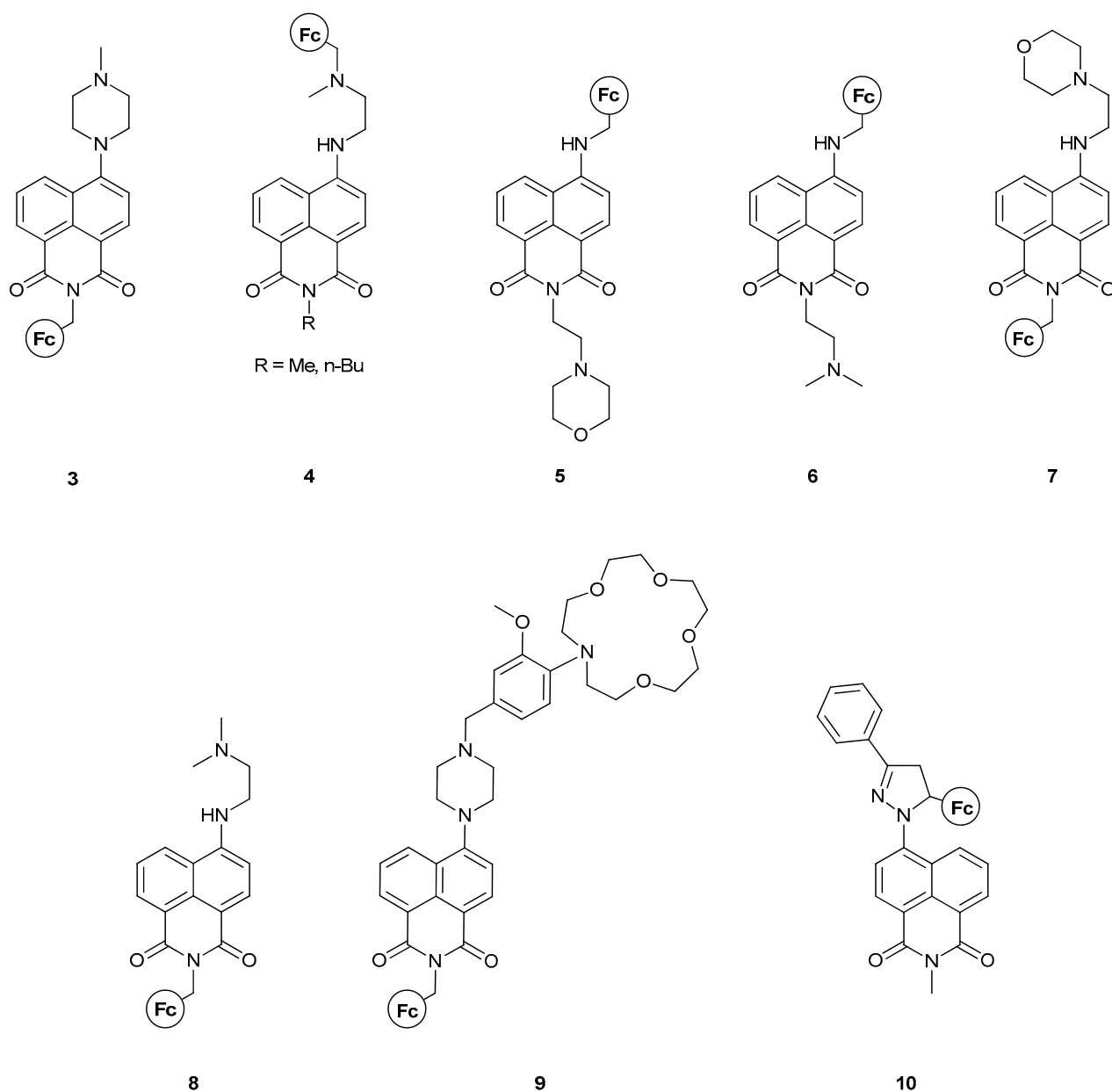


Figure 8. An assembly of naphthalimide-based MS-MLGs developed during the last decade from the group of Magri.

Compound **9** [37], featuring the “lab-on-a-molecule” design (the first one with an NA fluorophore scaffold), resembles the previous three compounds in that all are synthesized with the “electron-donor-spacer-fluorophore-spacer-proton-acceptor” motif. Moreover, it features an ion-receptor as an extra functional group and thus can serve as a multi-input logic gate. The molecule’s logical behavior was tested under acidic and oxidizing

conditions, with Na^+ ions present. Only when all three inputs were high was a record 25-fold fluorescent enhancement observed, even with the human eye; its quantum yield was of an order of magnitude greater than the group's previous results. Based on their results, we can highlight that this molecule could also act as an AND MLG in the presence of only H^+ and Fe^{3+} ions, pointing to this molecular design as a privileged motif for AND logic gates.

Along with 7 and 8, molecules 5 [17] and 6 [17] were also studied, which feature the regioisomers of the first two. In this case, no fluorescence enhancement was observed due to a negative electric field at the imine field, abetting the PET process. Overall, these two regioisomers fall short of a profound logic gate function, as, in all cases, the molecular design leads to excited state quenching and behaves as a PASS 0 logic gate.

Compounds 4 [38] and 10 [39] also bear a similar motif, where both the electron donor and proton acceptor are localized on the same side and on the back of the fluorophore. Compound 4 can feature either a methyl or a n-butyl group at the N-end of the NA moiety. Both molecules feature a lower fluorescence quantum yield compared to previous results, but the yield was still not insignificant. The study included time-resolved fluorescence spectroscopy and the authors compared their findings with previously designed molecules. As before, two AND logic gates were obtained, featuring a fourfold emission enhancement due to the ICT and PET quenching when both inputs are high. Compound 10, on the other hand, is not emissive in its initial form. Designed according to the "electron donor-spacer-fluorophore-receptor" format, upon oxidation of the Fc moiety, a 14-fold fluorescent enhancement is observed, which is then quenched upon H^+ addition. The result is a Fe^{3+} -enabled, H^+ -disabled INHIBIT logic gate. Theoretical calculations also confirmed that the switching mechanism is a PET process with the use of DFT methodology at the B3LYP/6-31+G(d,p) level of theory.

Tzeliou and Tzeli [18] studied theoretically, via DFT/TD-DFT calculations, the photophysical properties of a three-input AND molecular logic gate that presents an enhanced fluorescence spectrum. It was found that the geometry conformation at an N atom of the piperazine group is the key factor for the correct calculation of the absorption spectra of the calculated structures. Its geometry is between tetrahedral and planar, while changes in the corresponding CNCC dihedral angle of about 10 degrees can cause significant shifts in the main peak of the absorption spectra of up to 100 nm. They explained the unusually enhanced fluorescence of a MLG, while they concluded that molecular systems with N atoms, whose geometry is between planar and tetrahedral, can be ideal molecules in sensors and molecular logic gates. Their calculated absorption and emission spectra were in excellent agreement with the available experimental data [37].

Tzeliou and Tzeli [19] studied, via DFT and TD-DFT, the photophysical properties of metallocene-4-amino-1,8-naphthalimide-piperazine molecules (1-M^{2+}), and their oxidized and protonated derivatives (1-M^{3+} , $1\text{-M}^{2+}\text{-H}^+$, and $1\text{-M}^{3+}\text{-H}^+$), where $\text{M} = \text{Fe}, \text{Co},$ and Ni , employing three functionals, i.e., PBE0, TPSSh, and wB97XD. The calculated systems had not been investigated before. Also, the molecular system has the potential to be used as a sensor. Specifically, both the 1-Co^{2+} and 1-Co^{3+} can be used as a simple NOT molecular logic gate where the input is the protonation. Additionally, the $1\text{-Co}^{2+}\text{-H}^+$ can also be used as an NOT MLG, with the oxidation being the input. Finally, the 1-Co^{2+} can be considered as a two-input NAND MLG when the oxidation and the protonation are considered as inputs.

III. Fc-based MS-MLG containing other fused heterocycles as fluorophore.

The group of Magri has also reported on other MS-MLGs based on fused heterocycles with more extensive conjugated systems [40] (Figure 9). In these three molecules, the fluorophores are symmetric; thus, no regioisomers exist. In molecules 11 and 12, the perylenediimide (PDI) backbone affords a considerably longer conjugation, which is expected to alter the photophysics of the compound and its general logical function. Both compounds function as AND logic gates, where the inputs are the H^+ and Fe^{3+} ions. The quantum yields and emission enhancement are not special compared to previous reports,

but the PDI scaffold performs exceptionally well considering the fluorescence wavelength. The emission output is around 500 nm, excluding the presence of inner filter effects at high Fe^{3+} concentrations, and thus yielding a robust analytical tool. The authors showed the successful use of **12** in a polyurethane coating, which is able to detect premature corrosion.

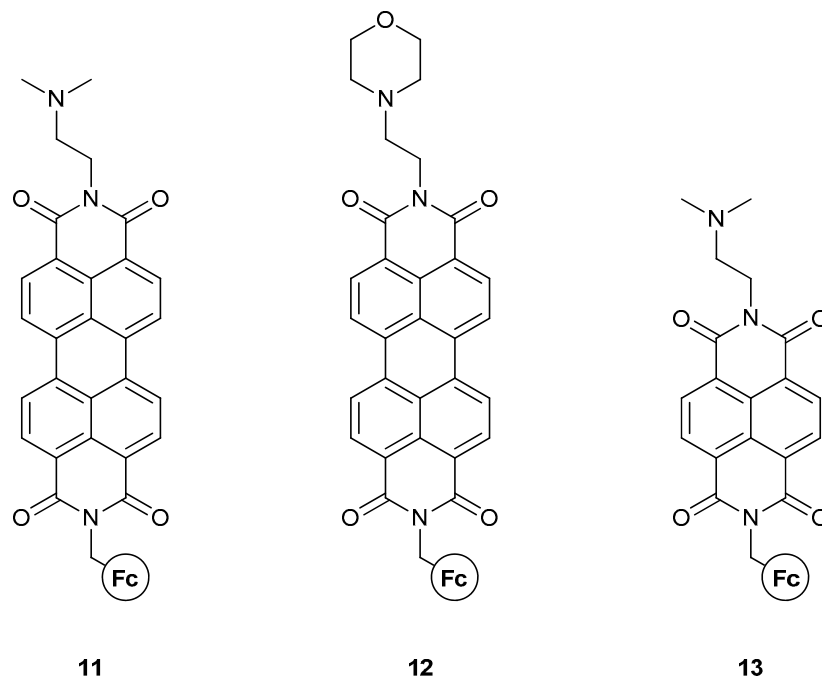


Figure 9. Magri's work on a ferrocene-based MLG featuring extensive polyaromatic systems as fluorophores.

Compound **13** [41] resembles **11**, but with a smaller polyaromatic system, similar to fluorophore. In contrast to previous molecular architectures, both **11** and **13** are modulated by PET mechanisms, rather than a combination of PET and ICT. For **13**, the naphthalenediimide (NDI) scaffold completely alters the logic function of the molecule, yielding a PASS-0 logic gate with H^+ and Fe^{3+} as inputs. The authors justified the results on the grounds of paramagnetic and/or inner filter effects, which NDI is very sensitive to.

Other interesting work, based on the use of fused aromatic rings as the fluorophores of the system, was carried out by the group of Thakur, as shown in Figure 10.

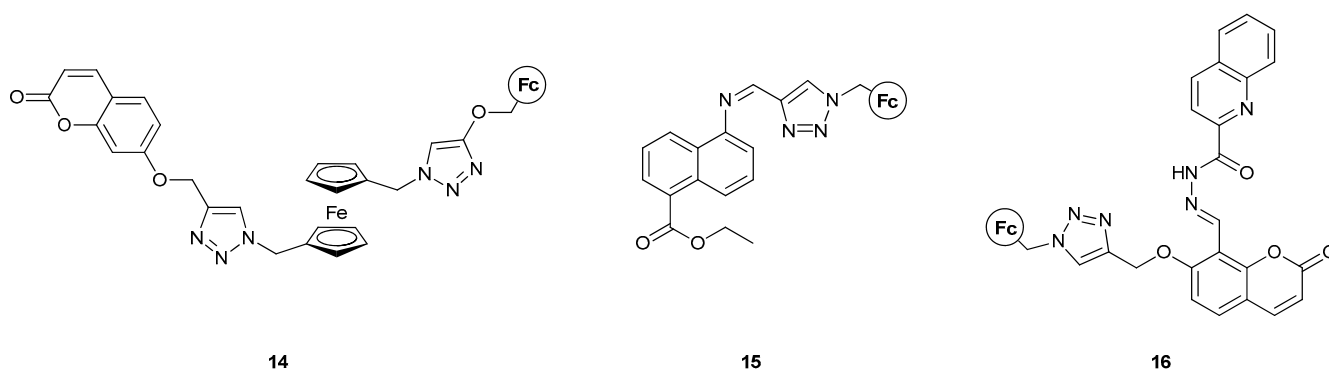


Figure 10. Three MS-MLGs developed by the group of Thakur featuring fused aromatic rings as the fluorophoring part of the molecule.

To the best of our knowledge, **14** [42] represents the first MLG containing two ferrocene moieties in the molecular scaffold, which can both be oxidized in the presence of Fe^{3+} , following the “redox_unit1–spacer1–receptor1–spacer2–redox_unit2–spacer3–recep-

tor2–spacer4–fluorophore” format. The fluorescence signal could be modulated by the combination of one cation binding event with the heavy metal Hg^{2+} and one chemical redox reaction where $\text{Fe}(\text{ClO}_4)_3$ was the oxidant and sodium L-ascorbate was the reducing agent. The logic function of **14** corresponds to an INHIBIT logic gate when either Fe^{3+} and Hg^{2+} or Fe^{3+} and LAS are used as inputs. When all three inputs are used, the result is a combinational NOR-AND logic circuit. It is important to note the geometrical rearrangement of the molecule, while ligating the Hg^{2+} ion and the constant increase in emissions despite the high concentrations of Fe^{3+} , which would otherwise decrease fluorescence due to the inner filter effects. Theoretical studies with DFT supported the quenching of a PET process between the Fc and coumarin moieties as the reason for emission enhancement. More specifically, DFT calculations were carried out using Gaussian 09 software at the B3LYP/def2-SVP/CPCM level of theory in acetonitrile for the optimization of geometry without any symmetry constraints, as well as TD-DFT calculations at the B3LYP/def2-SVP/CPCM level of theory in acetonitrile.

For compound **15** [43], a plethora of metal ions were used to test its UV-visible absorption, where only Hg^{2+} showed a significant effect. The molecule was shown to be an excellent mercury detector (limit of detection, LOD = 2.7 ppb), even with the human eye. The presence of mercury also enhanced the fluorescence output of the system, as it blocked the C=N bond isomerization upon excitation. It was further shown that H^+ also leads to fluorescence enhancement, which can be regulated in an ON-OFF manner with OH^- . INHIBIT and OR logic gates were developed, using H^+ and OH^- as inputs in the former, and H^+ and Hg^{2+} in the latter. These two logic gates were then further attached to form an INHIBIT–OR combinational gate. DFT calculations with the B3LYP functional were performed to reveal the structural and electronic parameters that control the responses of compound **15** toward Hg^{2+} and to optimize the geometry of the protonated species, while TD-DFT was also employed and CH_3CN was the solvent of choice.

Similarly, compound **16** [44] yielded a combinational AND-OR logic circuit with Fe^{3+} , Cu^{2+} and LAS as inputs. This probe was very specific toward Fe^{3+} via a reversible redox process, while it detected Cu^{2+} via irreversible oxidation. The addition of Fe^{3+} and Cu^{2+} ions resulted in the fluorescence emission of the probe showing a “turn-on” signal due to the inhibition of the PET process from a ferrocene donor unit to an excited-state fluorophore. A reducing agent, sodium L-ascorbate (LAS), is added and causes fluorescence “turn off” for Fe^{3+} due to PET process restoration, but this is not true for Cu^{2+} as it oxidizes the ferrocene unit to a ferrocenium ion with its concomitant reduction to Cu^+ , which further complexes with the probe. Absorption was perturbed only in the presence of Fe^{3+} , Cu^{2+} , and Cu^+ , where Cu^+ was shown to form a coordination compound with **16**. More specifically, the use of Fe^{3+} and LAS as inputs yielded an INHIBIT logic gate, while the use of Fe^{3+} and Cu^{2+} yielded an OR gate. The authors used these two ions as oxidizing agents rather than binding agents. Complexation–decomplexation of the Cu^+ ion could also regulate fluorescence emissions from the system. DFT calculations were performed using the B3LYP/LANL2DZ/conductor-like polarizable continuum model (CPCM) level in CH_3CN to obtain detailed theoretical aspects of the structural and electronic parameters of the probe before and after the oxidation and complexation with the corresponding metal ions.

IV. Fc-based MS-MLG containing other fluorophores.

Molecules based on ferrocene that exhibit logic behavior are ubiquitous, and thus many examples exist that do not fall into any of the previous categories. Such examples are presented in Figure 11 and will be discussed below.

In 2010, Wu et al. [45] reported the synthesis of compound **17** and exploited its excited states of metal-to-ligand charge transfer (MLCT), intraligand charge transfer (ILCT), ligand-to-ligand charge transfer (LLCT), and ligand-to-metal charge transfer (LM'CT), where M and M' indicate Pt and Fe, respectively. The multitude of different excited states was delicately used to produce a combinational AND-OR-NOT logic circuit. This three-input–four-output system involved alterations in the dominance of each excited state

in the presence of H^+ , Fe^{3+} , and Zn-powder. The four outputs were the emission peaks for the abovementioned states. The protonation of the pendant amine group, along with the oxidation/reduction of the Fc moiety, results in stark changes in the molecular orbitals, and therefore the ordering of the excited state, thus representing a handy way to modulate the emission properties of the system.

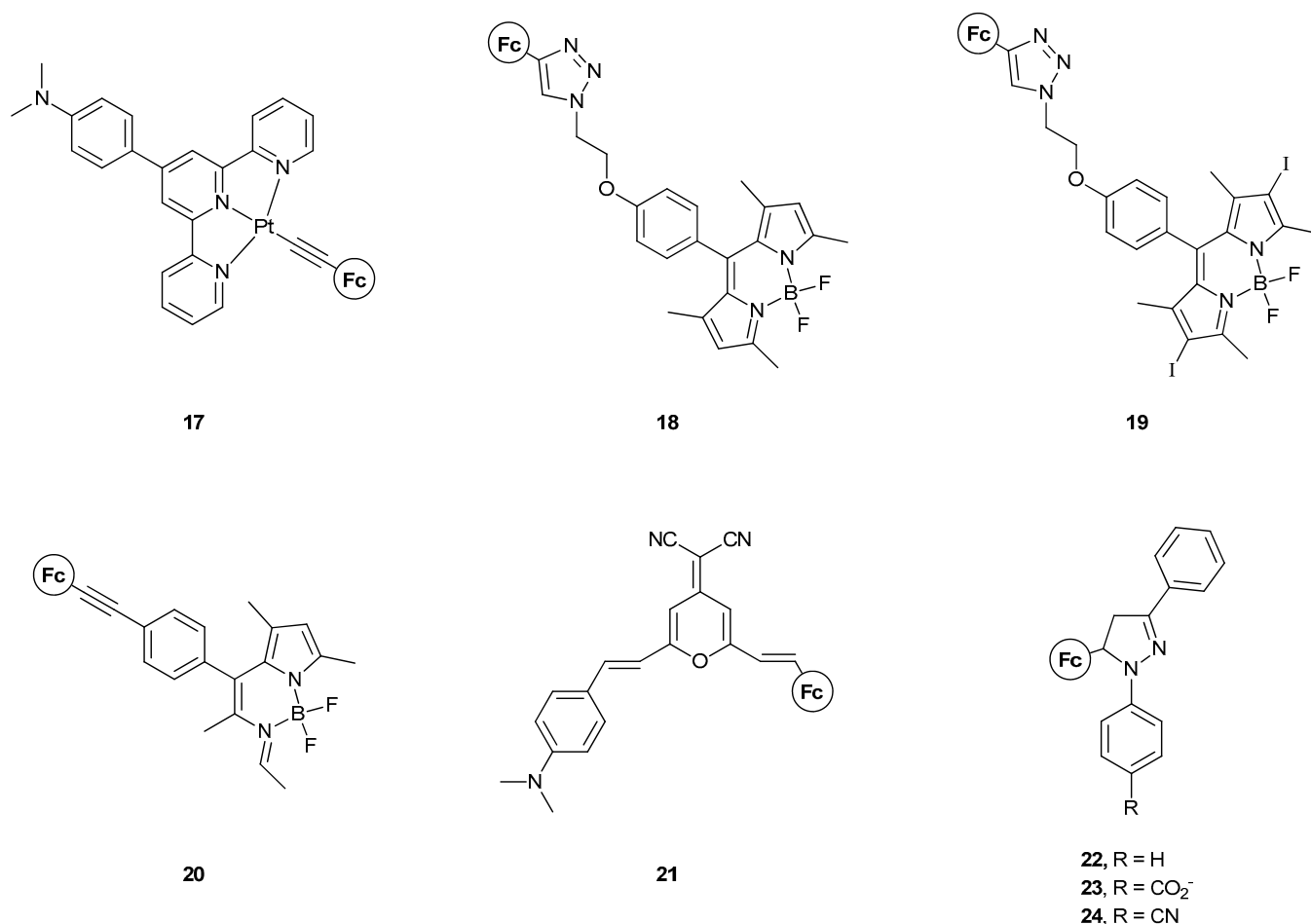


Figure 11. MS-MLGs based on ferrocene that feature other fluorophores that were not described in the previous three categories.

The groups of Wu, Wu, and Zhao reported, in 2016 [46], compounds 18–20, in which the dyads of Fc and Bodipy are present, and the Fc group acts as a modulator of Bodipy's excited states. Although not studied for their logic gate application, a very interesting study was conducted on their ON–OFF switch behavior with either electrochemical or chemical oxidation–reduction. Two mechanisms were found to be responsible for this behavior, PET, and triplet–triplet energy transfer, resulting in triplet state quenching. Upon oxidation of the Fc moiety, these are quenched and a fluorescence enhancement is observed. Compound 19 does not show such a switch functionality as the quenching effects are more intricate and lead to there being no triplet–triplet annihilation upconversion.

Zhu et al. [47] reported, one year later, compound 21, which also features an ON–OFF logic functionality, with both PET and ICT mechanisms taking place. Electrochemical modulation of the oxidation state of Fe in the Fc group results in a fine interplay between the two electron-transfer pathways, with Fe^{3+} leading to the fluorescent state.

In the same year, the group of Magri [48] studied compounds 22–24, where a spacer was included between the electron donor and the fluorophore, in comparison to Wu's previous example, where the spacer was between the fluorophore and receptor. An INHIBIT logic gate was developed, with Fe^{3+} and H^+ as inputs. All three compounds yielded a

high output only when Fe^{3+} was present. However, the region of emission was near where Fe^{3+} absorbs.

Dewangan et al. [49] used a solvent-free solid-state method to synthesize a 1,1'-unsymmetrical ferrocene-based turn-on fluorescent hydrazone molecular system. DFT calculations and a spectroscopic analysis were performed to establish the interaction behavior of the unsymmetrical ferrocene-based rhodaminyl organometallic receptor. The observations of significant intracellular metal recognition and imaging characteristics indicate their potential in applications involving the bioimaging of heavy metal ions. The fluorometric molecular compound was found to lead to an INHIBIT MLG, OR MLG, and a combinational logic operation. DFT calculations including the geometry optimization of the compounds under study were carried out in gas phase at the B3LYP/LANL2DZ level of theory.

Tamulis et al. [50] presented logic gates of molecular electronics digital computers, with maximal length of four nanometers and a maximal width of 2.5 nm. Light-driven logically controlled (OR, AND) molecular machines were composed of organic photoactive electron donor dithieno[3,2-b:2',3'-d]thiophene and ferrocene molecules, an electron-accepting tetracyano-indane molecule, and a moving azo-benzene molecular fragment. DFT and TD-DFT calculations were carried out at the B3PW91/6-311G level of the theory to obtain the absorption spectra of the designed molecular gates.

V. Fc-based MS-MLGs not in the other categories.

Tokunaga et al. [51] presented a practical procedure which combines aspects of classical electrostatics and DFT calculations to simplify the molecular shapes for device design. They applied this method to a library of biferrocenium dimers with a three-input junction. It was theoretically obtained that a covalently bonded parallelogram dimer responds to precisely six different patterns of nanoscale electric fields and can work correctly as a device cell in both AND and OR logic gates. This procedure was applied to quasi-square tetrametallic Ru complexes as well, and it was found that these complexes do not work as logic gates. This procedure expands the range of existing candidate molecules from squares to parallelograms and facilitates screening for implementation.

Alzahrani et al. [52] designed and synthesized a novel triphenylamine (TPA)-based sensor 1-(4-diphenylamino)phenyl)-3-(p-tolyl)thiourea (TTU) that exhibited reversible mechanochromic- and aggregation-induced emission enhancement (AIEE) properties. The AIEE active sensor was employed for the fluorometric detection of Fe^{3+} in aqueous medium, with high selectivity. The sensor showed a highly selective quenching response towards Fe^{3+} that is ascribed to its complex formation with paramagnetic Fe^{3+} . Subsequently, the TTU- Fe^{3+} complex acted as a fluorescence sensor for the detection of deferasirox (DFX). The subsequent addition of DFX to the TTU- Fe^{3+} complex led to the recovery of the fluorescence emission intensity of sensor TTU, which was attributed to the displacement of Fe^{3+} by DFX and the release of sensor TTU. DFT calculations were performed to understand the theoretical perspective of the interaction between sensor TTU and analyte Fe^{3+} .

In sum, although MS-MLG is the most studied family of molecular logic gates incorporating the Fc moiety, straightforward design principles remain unknown. This is understandable in terms of the synthetic difficulties, along with the newness of this field. Some basic guidelines exist that make some systems more privileged than others, i.e., the NA scaffold appears to be the best choice for an MS-MLG, as it can provide symmetry degeneracy or even be incorporated into a bigger aromatic scaffold. It should already be clear that the presence of the Fc group greatly enhances the redox properties of these molecules, and their synthetic tunability as well. Ferrocene can replace other redox-centers that are employed in the usual organic MLGs to further expand the library of MS-MLGs, and other metallocenes can also be incorporated. The present state represents a great chance for the experimental and theoretical community to join forces and systematically search for design principles.

2.3. Miscellaneous MLG Systems Using Ferrocene

The desirable characteristics of ferrocene make it a great addition to a system showing logic characteristics, even if it is not incorporated promptly. Many such systems exist [53–57], which mainly use ferrocene or its derivatives as external additives. Its electrochemical character makes it a proper input for the logic operation. Some informative are as follows. Liu et al. [58] used ferrocene–methanol as an input because of its ability to influence the system’s electrochemiluminescence. Yang et al. [59] reported on an indium tin oxide featuring ferrocene as an electroactive dye. Based on its diffusivity, an electrochemical MLG could be developed. Li and coworkers [60] used ferrocene as a reducing agent for an Au electrode, which, upon oxidation, would quench the electrochemiluminescence of the system.

In 2018, Magri published a short review where he presented the progress in molecular logic so far, more specifically focusing on molecules capable of sensing acidity and oxidizability. AND logic gates that provide a high fluorescence output when simultaneously protonated and oxidized were included, as well as molecules with three-input variants and molecules that function as INHIBIT logic gates. Photochemical concepts such as PET and ICT are used as the favorite design concepts. This review highlights the evolution of Pourbaix sensors with anthracene, pyrazoline, and naphthalimide fluorophores, while ferrocene is the electron donor mentioned in most molecules [61].

In 2021, Magri published a review paper on the evolution of fluorescence sensing at the University of Malta in the context of molecular-logic-based computation. PET was the design principle, while redox-driven switching was highlighted, as well as traditional acid-base and ion-binding phenomena. Cross-pollination with ICT further affords intelligent molecules, with properties classified according to the sophistication of the logic function from one-, two- and three-input systems including the concepts of Pourbaix sensors, lab-on-a-molecules and polymer tagged logic beads. There are references to an H⁺, Fe³⁺-driven AND logic gate, three-input AND logic gates, Lab-on-a-Molecules, and redox-driven INHIBIT logic gates, where either Fe or the ferrocene unit take part. Ferrocene was found in many of the molecules they studied as it is representative of electron donor units that can be singly oxidized [62].

All the above show that the very interesting behavior of ferrocene has led many researchers to incorporate it into various type of structures with different combinations of units and chemical elements, and to try out different numbers and types of inputs to synthesize and study MLGs with properties that make them prominent candidates for practical use. Finally, a summary of the previous experimental and theoretical MLG studies on compounds containing the ferrocene moiety is presented in Table 1.

Table 1. Summarized results of MLGs with Fc presented in this work.

Logic Operation	MS-MLG [Ref.] ^a	LC-MLG [Ref.] ^a
1-input		
YES	[52] (expt + th)	[23] (expt)
NOT	[19] (th)	[20] (expt + th); [22] (expt)
PASS	5 [17] (expt + th); 6 [17] (expt + th); 13 [41] (expt)	[20] (expt + th); [23] (expt + th)
2-input		
AND	3 [36] (expt); 4 [38] (expt); 7 [17] (expt + th); 8 [17] (expt + th); 9 [37] (expt); [18] (th); 11 [40] (expt); 12 [40] (expt); [50] (th); [51] (th); [30] (expt); [31] (expt); [32] (expt)	[22] (expt + th); [23] (expt + th); [26] (expt); [28] (expt); [60] (expt)
NAND	[19] (th)	[20] (expt + th); [60] (expt)
OR	15 [43] (expt); 16 [44] (expt + th); [50] (th); [51] (th)	[20] (expt + th); [21] (expt); [28] (expt); [60] (expt)

Table 1. Cont.

Logic Operation	MS-MLG [Ref.] ^a	LC-MLG [Ref.] ^a
NOR		[20] (expt + th); [60] (expt)
XOR		[20] (expt + th); [21] (expt); [22] (expt)
XNOR		[20] (expt + th)
INHIBIT	1 [34] (expt); 10 [39] (expt + th); 14 [42] (expt + th); 15 [43] (expt + th); 16 [44] (expt + th); 22–24 [48] (expt)	[24] (expt); [49] (expt + th); [60] (expt)
Combinational		
NOR-AND	1 [34]; 14 [42] (expt + th)	
INHIBIT-OR	15 [43] (expt + th); [49] (expt + th)	[49] (expt + th)
AND-OR	16 [44] (expt + th); [50] (expt + th); [51] (th)	
AND-OR-NOT	17 [45] (expt)	
AND-INHIBIT-YES		[58] (expt)
AND-INHIBIT-YES-IMPLICATION		[58] (expt)
ON/OFF		
	[33] (expt); [46] (expt); [47] (expt)	

^a expt: experimental; th: theory calculations.

3. MLGs including a Metal Cation without the Ferrocene Moiety

Akkaya et al. [63] experimentally studied multivalent–multitopic bodipy derivatives, with metal ion–ligand pairs based on known affinities, and thus PET and ICT processes could be manipulated as desired. They obtained a molecular equivalent of a three-input AND logic gate exploiting the differential binding affinities of metal ions for different ligands. This resulted in a range of signals that are useful in molecular logic design, and offered enticing potential for multianalyte chemosensors. Tzeli et al. [64,65] theoretically studied, via DFT and TD-DFT, the photophysical processes of a styryl–bodipy derivative that acts as a three-receptor fluorophore and is a candidate for a three-input AND molecular logic gate in the emission mode. The inputs were the Ca^{2+} , Zn^{2+} , and Hg^{2+} cations that present high selectivity, i.e., they were complexed in specific part of the molecule. Different solvents were considered for the computational study and it was found that the molecule can act as a three-input AND MLG only in specific solvent conditions. The photophysical properties of the MLG were explained, while the cruciality of solvent selection to allow for a species to act as an MLG candidate was highlighted.

Velmurugan et al. [66] synthesized an amine dangled Schiff base quinoline–morpholine conjugate (QMC), which selectively detects Pb^{2+} -ions with large blue-shift fluorescent emissions through ICT processes. The QMC and QMC + Pb^{2+} complex structures were optimized using DFT at the B3LYP/LANL2DZ level of theory. An INHIBIT molecular logic function was constructed by using Pb^{2+} and EDTA as chemical inputs.

Bahta and Ahmed [67] theoretically studied a novel colorimetric and ratiometric fluorescent chemosensor for Hg^{2+} ions, employing DFT (B3LYP/6–31G(d)LANL2DZ_{Hg}) and TD-DFT (CAM-B3LYP/6–31G(d)LANL2DZ_{Hg}).

Fu et al. [68] designed and synthesized a reversible dual-channel sensor for the detection of Cu^{2+} . Calculations were performed on the molecules of the sensor and the sensor with Cu^{2+} using DFT at the B3LYP/6-311 + G* level of theory. Fluorescence changes in the sensor upon the addition of Cu^{2+} and EDTA were applied as an ultrasensitive IMPLICATION logic gate at the molecular level.

Mukherjee and Betal [69] synthesized a new, simple, small-molecule hydrazone from the reaction of pyrene-1-aldehyde and 2-hydrazinobenzoic acid. It was investigated as a reversible, turn-on luminescent chemosensor for copper ion (Cu^{2+}) in an aqueous environment via DFT(B3LYP/6–31+G(d,p)_{C,N,O} 6–31+G_H LANL2DZ_{Cu}). TD-DFT calculations

were also carried out using DMSO solvent. In the presence of Cu^{2+} , the ligand exhibits a reversible change in emission pattern with oxalate ($\text{C}_2\text{O}_4^{2-}$), and thus Cu^{2+} and $\text{C}_2\text{O}_4^{2-}$ could be used as chemical inputs on a molecular 'INHIBIT' logic gate.

Ray et al. [70] studied the dye-containing Cu(II)-Schiff base complex for the easy monitoring of D-penicillamine (D-PA), a tri-functional organic compound (thiol, amine, and carboxylic acid) which is used as a chelating drug for many serious diseases, such as Wilson's disease. The synthesized Cu(II)-salicylaldehyde rhodamine B hydrazone complex was characterized with Fourier-transform infrared spectroscopy (FTIR), nuclear magnetic resonance (NMR), mass spectrometry, UV-Vis, and fluorescence titrations, while DFT calculations were carried out to optimize the crystal structure of the complex. An NAND-type molecular logic gate was developed.

All the studies presented above indicate that, while ferrocene is very effective as an electron donor, there are plenty of molecules that exhibit interesting behavior: they detect ions (in most cases) and act as MLGs. Thus, there is a wide variety of molecules that could be explored to effectively act as the electron donor and result in various types of MLGs. The most effective electron donors can be found in this way and categorized depending on the system under study and the properties we aim for the system to have.

4. Computational Methodologies Used for MLG Prediction

In the last decade, computational chemistry has been applied for the evaluation of compounds as MLG candidates. Their geometries, not only of their global minimum structures but also of their local minimum isomers and conformers, are computed via quantum chemical calculations. Additionally, their electronic structure, bonding, and magnetic properties, and their absorption, emission, infrared (IR), and electron paramagnetic resonance (EPR) spectra, are also predicted [71–78]. Furthermore, the plot of the frontier molecular orbitals can assist in explaining the photophysical and photochemical properties of the metallic complexes and their reaction properties, while useful information can be obtained regarding the prediction of favorable pathways for their synthesis, their catalytic role in synthetic reactions with the activation of certain bonds, etc. [71–82]. Furthermore, calculations can explain how the molecules respond to changes in their environment, such as the presence of various ions, neutral species, pHs, temperatures, and viscosities.

The correct calculation of the electronic structure and of both the absorption and emission spectra of the molecules is crucial for characterizing a molecule as an MLG candidate. When there are experimental data regarding the absorption or fluorescence spectrum of an MLG candidate, researchers search for an appropriate methodology to reproduce the experimental data. However, the question is how someone can correctly predict the MLG candidates. Usually, except theoreticians, many non-experts use one of the many user-friendly software packages which apply sophisticated quantum-chemical methods to calculate the geometry, the electronic structure, and both the absorption and fluorescence spectra. However, very often, errors occur due to misunderstandings of the methodologies of computational chemistry, the technical settings and the technical details of the calculations, and the technical aspects of the quantum chemical methodologies. In what follows, the commonly used theoretical methodologies are described and recommendations are made for the accurate prediction of MLG candidates.

The most popular methodology is DFT, as it is less time-consuming compared to other methodologies, it is not difficult to use, at least at a basic level, and accurate data can be obtained when applied cautiously. The choice of functional and basis sets for the calculations is very important and varies depending on the problem. If not chosen appropriately, the results will be significantly affected. For this reason, a preliminary investigation is recommended, where different combinations of functionals and basis sets will be applied concerning the parameters of geometry and the absorption spectra. The obtained data should be compared with either accurate multireference techniques or the experimental data. This process will lead to the determination of the most appropriate functional and basis sets for the theoretical calculations.

The most popular functional used in computational chemistry is B3LYP [83], which provides generally satisfactory results regarding geometry and can usually predict the absorption spectra correctly. B3LYP has been used for theoretical calculations of ferrocene [16]. However, PBE0 is the functional that has yielded the most accurate results in the prediction of the ferrocene properties [19]. The Minnesota family functionals M06 [84] have also become very popular, while long-range corrected hybrid functionals wB97, wB97X, wB97X-D, and wB97X-2 could be used as well. These include a full Hartree–Fock exchange at long-range interelectron distances, leading to a reduction in the self-interaction errors. If dispersion correction is necessary in either B3LYP or PBE0, it can be properly added with the use of semiempirical corrections, such as Grimme’s -D3 corrections, which are available for both [85].

Regarding the basis sets, depending on the size of the system, an augmented double zeta quality basis set is appropriate for large complexes of about 100–150 atoms. For instance, the 6–31+G(d,p) family of basis sets [86], combined with a basis set including pseudopotentials such as LANL2DZ for the metals [87], or the Def2-SVP [88] for all atoms, is a good choice. For smaller complexes, an augmented triplet quality basis set, such as def-2TZVP [88] or aug-cc-pVTZ(-PP) [89,90], would work accurately.

The MLG compounds are solved in a variety of solvents. In calculations, the solvent can be included via the dielectric constant (implicitly), [91] as molecules (explicitly), or as dielectric constant and molecules simultaneously (hybrid model). The inclusion of a solvent via dielectric constant does not significantly affect the geometry or the spectra. However, in some cases, mainly in polar solvents, the gas phase spectra can be shifted when the solvent is added implicitly. On the contrary, the explicit inclusion of one or more solvent molecules may significantly affect the spectra [18]. Furthermore, the linear response corrections [92] are important to consider, especially when the solvent is only added implicitly. They can lead to shifts in the absorption peaks, mainly the emission peaks, and especially in cases where charge transfer excitations or de-excitations are involved.

Another option for the accurate calculation of the absorption and emission spectra is the application of an accurate *ab initio* methodology. In general, while DFT methodologies calculate the geometry correctly, when it comes to the calculation of the excited electronic states, difficulties arise in their accurate prediction with the use of DFT. In this case, geometries can be calculated with an appropriate combination of functional and basis sets, and then the electronic structure should be calculated via a multireference *ab initio* methodology. A very good choice is the complete active space self-consistent field method (CASSCF) [93], followed by the second-order perturbation treatment (CASPT2), or by a second-order perturbation treatment of the dynamic electron correlation (NEVPT2 [94]).

Finally, both population analysis and the plot of the frontier molecular orbital can provide useful information regarding charge or electron transfer processes. Mulliken population analysis is extensively used, mainly because it is the default analysis in many computational programs; however, Mulliken charges may show basis set dependency or an underestimation of the ionic character [95,96]. On the other hand, the natural population analysis (NPA) method is almost independent of the basis set but can also present some problems [97] and overestimate the ionic character of the atoms [98]. Other population analyses includes the Hirshfield and its extension CM5 model [99].

Overall, computational chemistry is a powerful tool for predicting compounds’ potential as MLG candidates, while assisting in the explanation of the photochemical and photophysical properties of the compounds.

5. Conclusions and Future Perspectives

In the last four decades, much research has been conducted to investigate and design molecular systems that can process information. Additionally, many reviews have been written reporting the latest advancements on this topic, while they provide novel ideas and discuss different possible future directions [10,100–107]. In the coming decade, many applications are expected to be developed in a variety of research fields, ranging from

medicine, in which the MLGs will be applied in photodynamic therapy, for intracellular uses, and in biomedical applications [108,109], to material science [110], and, of course, information security, where the semiconductors which are used in the Information Technology (IT) industry will be replaced by MLGs [10]. Note that many issues that occur when semiconductors are applied in nano-dimensions via the use of MLGs, as they will be overwhelmed [10]. Furthermore, MLGs can be used in environmental analysis, for instance, in water quality monitoring and heavy metal ion detection, as well as for securing food safety [111]. In sum, MLGs have broad development potential; studies on MLGs will remain active in the coming decades, and researchers' creativity can significantly increase the applications of MLGs.

Significant advances have been made in the development of Fc receptors capable of selectively sensing metal cations [111]. Ferrocene can easily donate an electron in molecular systems designed according to the principles of modular photoelectron transfer. The ferrocene–ferrocenium couple is a versatile redox switch [112] and can easily be used as an input in the MLGs. The redox chemistry of Fc, in conjunction with the stability of the molecular systems, their solubility in solvents of varying polarity, and their ease of functionalization can lead to the design of many ferrocene-based catalysts, with many applications in nanomedicine, biological sensing, materials science, etc.

Author Contributions: C.E.T.: Investigation, data curation, formal analysis, writing—original draft preparation; K.P.Z.: investigation, data curation, formal analysis, visualization, writing—original draft preparation; D.T.: conceptualization, investigation, methodology, administration, supervision, writing—original draft, review, and editing. All authors have read and agreed to the published version of the manuscript.

Funding: C.E.T. acknowledges CSTM project for financial support. K.P.Z. acknowledges Bodossaki Institution for financial support, (MSc scholarship 2023–2024).

Data Availability Statement: No new data were created or analyzed in this study. Data sharing is not applicable to this article.

Conflicts of Interest: The authors declare no conflicts of interest.

References

1. Balzani, V.; Credi, A.; Venturi, M. *Molecular Devices and Machines Concepts and Perspectives for the Nanoworld*, 2nd ed.; WILEY-VCH Verlag GmbH & Co. KGaA: Weinheim, Germany, 2008; pp. 259–275.
2. Tzeliou, C.E.; Tzeli, D. *Logic Gates and Molecular Logic Gates*; Encyclopedia MDPI: Basel, Switzerland, 2024. Available online: <https://encyclopedia.pub/entry/56522> (accessed on 30 March 2024).
3. All about Circuits (Multiple-Input Gates). Available online: <https://www.allaboutcircuits.com/textbook/digital/chpt-3/multiple-input-gates/> (accessed on 29 March 2024).
4. de Silva, P.A.; Gunaratne, N.H.Q.; McCoy, C.P. A molecular photoionic AND gate based on fluorescent signaling. *Nature* **1993**, *364*, 42–44. [[CrossRef](#)]
5. de Silva, A.P.; Rupasinghe, R.A.D.D. A new class of fluorescent pH indicators based on photo-induced electron transfer. *J. Chem. Soc. Chem. Commun.* **1985**, 1669–1670. [[CrossRef](#)]
6. Huston, M.E.; Akkaya, E.U.; Czarnik, A.W. Chelation Enhanced Fluorescence Detection of Non-Metal Ions. *J. Am. Chem. Soc.* **1989**, *111*, 8735–8737. [[CrossRef](#)]
7. Hosseini, M.W.; Blacker, A.J.; Lehn, J.-M. Multiple molecular recognition and catalysis. A multifunctional anion receptor bearing an anion binding site, an intercalating group, and a catalytic site for nucleotide binding and hydrolysis. *J. Am. Chem. Soc.* **1990**, *112*, 3896–3904. [[CrossRef](#)]
8. Van Arman, S.A.; Czarnik, A.W. Chemical communication of enzymatic ATP hydrolysis using a fluorescent chemosensor. *Supramolec. Chem.* **1993**, *1*, 99–101. [[CrossRef](#)]
9. Aviram, A. Molecules for Memory, Logic, and Amplification. *J. Am. Chem. Soc.* **1988**, *110*, 5687–5692. [[CrossRef](#)]
10. Erbas-Cakmak, S.; Kolemen, S.; Sedgwick, A.C.; Gunnlaugsson, T.; James, T.D.; Yoon, J.; Akkaya, E.U. Molecular logic gates: The past, present and future. *Chem. Soc. Rev.* **2018**, *47*, 2228–2248. [[CrossRef](#)] [[PubMed](#)]
11. Kealy, T.; Pauson, P. A New Type of Organo-Iron Compound. *Nature* **1951**, *168*, 1039–1040. [[CrossRef](#)]
12. Wilkinson, G.; Rosenblum, M.; Whiting, M.C.; Woodward, R.B. The structure of iron bis-cyclopentadienyl. *J. Am. Chem. Soc.* **1952**, *74*, 2125–2126. [[CrossRef](#)]
13. Scott, D.R.; Becker, R.S. Comprehensive Investigation of the Electronic Spectroscopy and Theoretical Treatments of Ferrocene and Nickelocene. *J. Chem. Phys.* **1961**, *35*, 516–531; Erratum in *Commun. J. Chem. Phys.* **1961**, *35*, 2246–2247. [[CrossRef](#)]

14. Armstrong, A.T.; Smith, F.; Elder, E.; McGlynn, S.P. Electronic Absorption Spectrum of Ferrocene. *J. Chem. Phys.* **1967**, *46*, 4321–4328. [[CrossRef](#)]
15. Sohn, Y.S.; Hendrickson, D.N.; Hart Smith, J.; Gray, H.B. Single-crystal electronic spectrum of ferrocene at 4.2 °K. *Chem. Phys. Lett.* **1970**, *6*, 499–501. [[CrossRef](#)]
16. Salzner, U. Quantitatively Correct UV-vis Spectrum of Ferrocene with TDB3LYP. *J. Chem. Theory Comput.* **2013**, *9*, 4064–4073. [[CrossRef](#)] [[PubMed](#)]
17. Spiteri, J.C.; Denisov, S.A.; Jonusauskas, G.; Klejna, S.; Szaciłowski, K.; McClenaghan, N.D.; Magri, D.C. Molecular engineering of logic gate types by module rearrangement in ‘Pourbaix Sensors’: The effect of excited-state electric fields. *Org. Biomol. Chem.* **2018**, *16*, 6195–6201. [[CrossRef](#)] [[PubMed](#)]
18. Tzeliou, C.E.; Tzeli, D. 3-input AND molecular logic gate with enhanced fluorescence output: The key atom for the accurate prediction of the spectra. *J. Chem. Inf. Model.* **2022**, *62*, 6436–6448. [[CrossRef](#)] [[PubMed](#)]
19. Tzeliou, C.E.; Tzeli, D. Metallocene-naphthalimide derivatives: The effect of geometry, DFT methodology, and transition metals on absorption spectra. *Molecules* **2023**, *28*, 3565. [[CrossRef](#)] [[PubMed](#)]
20. Liu, R.; Han, Y.; Sun, F.; Khatri, G.; Kwon, J.; Nickle, C.; Wang, L.; Wang, C.-K.; Thompson, D.; Li, Z.-L.; et al. Stable Universal 1- and 2-Input Single-Molecule Logic Gates. *Adv. Mater.* **2022**, *34*, 2202135. [[CrossRef](#)] [[PubMed](#)]
21. Matsui, J.; Abe, K.; Mitsuishi, M.; Aoki, A.; Miyashita, T. Quasi-Solid-State Optical Logic Devices Based on Redox Polymer Nanosheet Assembly. *Langmuir* **2009**, *25*, 11061–11066. [[CrossRef](#)]
22. Afrasiabi, R.; Kraatz, H.-B. Rational Design and Application of a Redox-Active, Photoresponsive, Discrete Metallogelator. *Chem. Eur. J.* **2015**, *21*, 7695–7700. [[CrossRef](#)] [[PubMed](#)]
23. Vella Refalo, M.; Farrugia, N.V.; Johnson, A.D.; Klejna, S.; Szaciłowski, K.; Magri, D.C. Fluorimetric naphthalimide-based polymer logic beads responsive to acidity and oxidizability. *J. Mater. Chem. C* **2019**, *7*, 15225–15232. [[CrossRef](#)]
24. Zerafa, N.; Cini, M.; Magri, D.C. Molecular engineering of 1,3,5-triaryl-2-pyrazoline fluorescent logic systems responsive to acidity and oxidisability and attachment to polymer beads. *Mol. Syst. Des. Eng.* **2021**, *6*, 93–99. [[CrossRef](#)]
25. Liu, Y.; Offenhäusser, A.; Mayer, D. Molecular rectification in metal–bridge molecule–metal junctions. *Phys. Status Solidi A Appl. Mater. Sci.* **2010**, *207*, 891–897. [[CrossRef](#)]
26. Frasconi, M.; Mazzei, F. Electrochemically Controlled Assembly and Logic Gates Operations of Gold Nanoparticle Arrays. *Langmuir* **2012**, *28*, 3322–3331. [[CrossRef](#)] [[PubMed](#)]
27. Matsui, J.; Abe, K.; Mitsuishi, M.; Aoki, A.; Miyashita, T. Molecular Optical Switch Based on Polymer Nanosheet Assembly Operated at Visible Wavelength. *Chem. Lett.* **2011**, *40*, 816–817. [[CrossRef](#)]
28. Trasobares, J.; Martín-Romano, J.C.; Khaliq, M.W.; Ruiz-Gómez, S.; Foerster, M.; Niño, M.Á.; Pedraz, P.; Dappe, Y.J.; de Ory, M.C.; García-Pérez, J.; et al. Hybrid molecular graphene transistor as an operando and optoelectronic platform. *Nat. Commun.* **2023**, *14*, 1381. [[CrossRef](#)]
29. Hernández-Ortiz, O.J.; Cerón-Castelán, J.E.; Muñoz-Pérez, F.M.; Salazar-Pereda, V.; Ortega-Mendoza, J.G.; Veloz-Rodríguez, M.A.; Lobo-Guerrero, A.; Espinosa-Roa, A.; Rodríguez-Rivera, M.A.; Vázquez-García, R.A. Synthesis, optical, electrochemical, and magnetic properties of new ferrocenyl chalcone semiconductors for optoelectronic applications. *J. Mater. Sci. Mater. Electron.* **2020**, *31*, 3342–3353. [[CrossRef](#)]
30. Fang, C.-J.; Li, C.-Y.; Fu, X.-F.; Yue, Y.-F.; Yan, C.-H. Redox-Active Fluorescent Molecular Switch to Realize AND Logic Function. *Chin. J. Inorg. Chem.* **2008**, *24*, 1832–1836.
31. Farrugia, T.J.; Magri, D.C. ‘Pourbaix sensors’: A new class of fluorescent pE–pH molecular AND logic gates based on photoinduced electron transfer. *New J. Chem.* **2013**, *37*, 148–151. [[CrossRef](#)]
32. Magri, D.C.; Camilleri Fava, M.; Mallia, C.J. A sodium-enabled ‘Pourbaix sensor’: A three-input AND logic gate as a ‘lab-on-a-molecule’ for monitoring Na⁺, pH and pE. *Chem. Commun.* **2014**, *50*, 1009–1011. [[CrossRef](#)]
33. Zhu, W.; Song, L.; Yang, Y.; Tian, H. Novel Bisthienylethene Containing Ferrocenyl-Substituted Naphthalimide: A Photo- and Redox Multi-Addressable Molecular Switch. *Chem. Eur. J.* **2012**, *18*, 13388–13394. [[CrossRef](#)]
34. Li, M.; Guo, Z.; Zhu, W.; Marken, F.; James, T.D. A redox-activated fluorescence switch based on a ferrocene–fluorophore–boronic ester conjugate. *Chem. Commun.* **2015**, *51*, 1293–1296. [[CrossRef](#)]
35. Dong, J.; Hu, J.; Baigude, H.; Zhang, H. A novel ferrocenyl–naphthalimide as a multichannel probe for the detection of Cu(II) and Hg(II) in aqueous media and living cells. *Dalton Trans.* **2018**, *47*, 314–322. [[CrossRef](#)]
36. Spiteri, J.C.; Schembri, J.S.; Magri, D.C. A naphthalimide-based ‘Pourbaix sensor’: A redox and pH driven AND logic gate with photoinduced electron transfer and internal charge transfer mechanisms. *New J. Chem.* **2015**, *39*, 3349–3352. [[CrossRef](#)]
37. Scerri, G.J.; Spiteri, J.C.; Mallia, C.J.; Magri, D.C. A lab-on-a-molecule with an enhanced fluorescent readout on detection of three chemical species. *Chem. Commun.* **2019**, *55*, 4961–4964. [[CrossRef](#)]
38. Johnson, A.D.; Paterson, K.A.; Spiteri, J.C.; Denisov, S.A.; Jonusauskas, G.; Tron, A.; McClenaghan, N.D.; Magri, D.C. Water-soluble naphthalimide-based ‘Pourbaix sensors’: pH and redox-activated fluorescent AND logic gates based on photoinduced electron transfer. *New J. Chem.* **2016**, *40*, 9917–9922. [[CrossRef](#)]
39. Sammut, D.; Bugeja, N.; Szaciłowski, K.; Magri, D.C. Molecular engineering of fluorescent bichromophore 1,3,5-triaryl- Δ^2 -pyrazoline and 4-amino-1,8-naphthalimide molecular logic gates. *New J. Chem.* **2022**, *46*, 15042–15051. [[CrossRef](#)]
40. Scerri, G.J.; Spiteri, J.C.; Magri, D.C. Pourbaix sensors in polyurethane molecular logic-based coatings for early detection of corrosion. *Mater. Adv.* **2021**, *2*, 434–439. [[CrossRef](#)]

41. Grech, J.; Spiteri, J.C.; Scerri, G.J.; Magri, D.C. Molecular logic with ferrocene-rylene conjugates: A comparison of naphthalenediimide, naphthalimide and perylene diimide Pourbaix sensor designs. *Inorganica Chim. Acta* **2023**, *544*, 121176. [[CrossRef](#)]
42. Bhatta, S.R.; Bheemireddy, V.; Thakur, A. A Redox-Driven Fluorescence “Off-On” Molecular Switch Based on a 1,1'-Unsymmetrically Substituted Ferrocenyl Coumarin System: Mimicking Combinational Logic Operation. *Organometallics* **2017**, *36*, 829–838. [[CrossRef](#)]
43. Bhatta, S.R.; Mondal, B.; Vijaykumar, G.; Thakur, A. ICT-Isomerization-Induced Turn-On Fluorescence Probe with a Large Emission Shift for Mercury Ion: Application in Combinational Molecular Logic. *Inorg. Chem.* **2017**, *56*, 11577–11590. [[CrossRef](#)] [[PubMed](#)]
44. Karmakar, M.; Bhatta, S.R.; Giri, S.; Thakur, A. Oxidation-Induced Differentially Selective Turn-On Fluorescence via Photoinduced Electron Transfer Based on a Ferrocene-Appended Coumarin–Quinoline Platform: Application in Cascaded Molecular Logic. *Inorg. Chem.* **2020**, *59*, 4493–4507. [[CrossRef](#)] [[PubMed](#)]
45. Liu, X.-Y.; Han, X.; Zhang, L.-P.; Tung, C.-H.; Wu, L.-Z. Molecular logic circuit based on a multi-state mononuclear platinum(ii) terpyridyl complex. *Phys. Chem. Chem. Phys.* **2010**, *12*, 13026–13033. [[CrossRef](#)] [[PubMed](#)]
46. Wu, X.; Wu, W.; Cui, X.; Zhao, J.; Wu, M. Preparation of Bodipy–ferrocene dyads and modulation of the singlet/triplet excited state of bodipy via electron transfer and triplet energy transfer. *J. Mater. Chem. C* **2016**, *4*, 2843–2853. [[CrossRef](#)]
47. Yang, J.; Li, M.; Kang, L.; Zhu, W. A luminescence molecular switch via modulation of PET and ICT processes in DCM system. *Sci. China Chem.* **2017**, *60*, 607–613. [[CrossRef](#)]
48. Scerri, G.J.; Cini, M.; Schembri, J.S.; da Costa, P.F.; Johnson, A.D.; Magri, D.C. Redox-Enabled, pH-Disabled Pyrazoline–Ferrocene INHIBIT Logic Gates. *Chem. Phys. Chem.* **2017**, *18*, 1742–1745. [[CrossRef](#)] [[PubMed](#)]
49. Dewangan, S.; Barik, T.; Halder, B.; Mishra, A.; Dhiman, R.; Sasamori, T.; Chatterjee, S. Rhodamine tethered 1,1'-unsymmetrical ferrocene functionalization: Metal sensing, cell imaging and logic gate properties. *J. Organomet. Chem.* **2021**, *948*, 121922. [[CrossRef](#)]
50. Tamulis, A.; Tamulienė, J.; Tamulis, V.; Ziriakoviene, A. Quantum Mechanical Design of Molecular Computers Elements Suitable for Self-Assembling to Quantum Computing Living Systems. *Solid State Phenom.* **2004**, *97–98*, 173–180. [[CrossRef](#)]
51. Tokunaga, K.; Odate, F.; Asami, D.; Tahara, K.; Sato, M. A Theoretical Procedure Based on Classical Electrostatics and Density Functional Theory for Screening Non-Square-Shaped Mixed-Valence Complexes for Logic Gates in Molecular Quantum-Dot Cellular Automata. *Bull. Chem. Soc. Jpn.* **2021**, *94*, 397–403. [[CrossRef](#)]
52. Alzahrani, A.; Omama Khan, K.; Rafique, S.; Hasher, I.; Khadija; Khan, A.M.; Shahzad, S.A. Theoretical and experimental studies on mechanochromic triphenylamine based fluorescent “ON-OFF-ON” sensor for sequential detection of Fe³⁺ and deferasirox. *Spectrochim. Acta A Mol. Biomol. Spectrosc.* **2023**, *297*, 122745. [[CrossRef](#)] [[PubMed](#)]
53. Liang, J.; Li, M.; Lu, Y.; Yao, H.; Liu, H. An enzymatic calculation system based on electrochemiluminescence and fluorescence of luminol and cyclic voltammetry of ferrocene methanol. *Biosens. Bioelectron.* **2018**, *118*, 44–50. [[CrossRef](#)] [[PubMed](#)]
54. Wu, K.; Hou, Y.-J.; Lu, Y.-L.; Fan, Y.-Z.; Fan, Y.-N.; Yu, H.-J.; Li, K.; Pan, M.; Su, C.-Y. Redox-Guest-Induced Multimode Photoluminescence Switch for Sequential Logic Gates in a Photoactive Coordination Cage. *Chem. Eur. J.* **2019**, *25*, 11903. [[CrossRef](#)] [[PubMed](#)]
55. Zhai, Z.; Shan, X.; Li, M.; Liu, Y.; Yang, F.; Wang, F.; Tian, Z.; Shi, K.; Yao, H. Multiple stimuli-switchable electrocatalysis and logic gates of l-cysteine based on P(DEA-co-VPBA) hydrogel films. *Mol. Catal.* **2023**, *546*, 113273. [[CrossRef](#)]
56. Liang, J.; Yu, X.; Yang, T.; Li, M.; Shen, L.; Jin, Y.; Liu, H. A complicated biocomputing system based on multi-responsive P(NIPAM-co-APBA) copolymer film electrodes and electrocatalysis of NADH. *Phys. Chem. Chem. Phys.* **2017**, *19*, 22472–22481. [[CrossRef](#)] [[PubMed](#)]
57. Wei, W.; Li, J.; Yao, H.; Shi, K.; Liu, H. A versatile molecular logic system based on Eu(iii) coordination polymer film electrodes combined with multiple properties of NADH. *Phys. Chem. Chem. Phys.* **2020**, *22*, 22746–22757. [[CrossRef](#)] [[PubMed](#)]
58. Lian, W.; Yu, X.; Wang, L.; Liu, H. Biomacromolecular Logic Devices Based on Simultaneous Electrocatalytic and Electrochemiluminescence Responses of Ru(bpy)₃²⁺ at Molecularly Imprinted Polymer Film Electrodes. *J. Phys. Chem. C* **2015**, *119*, 20003–20010. [[CrossRef](#)]
59. Zhu, L.; Yu, L.; Yang, X. Electrochemical-Based DNA Logic Devices Regulated by the Diffusion and Intercalation of Electroactive Dyes. *ACS Appl. Mater. Interfaces* **2021**, *13*, 42250–42257. [[CrossRef](#)] [[PubMed](#)]
60. Li, X.; Sun, L.; Ding, T. Multiplexed sensing of mercury(II) and silver(I) ions: A new class of DNA electrochemiluminescent-molecular logic gates. *Biosens. Bioelectron.* **2011**, *26*, 3570–3576. [[CrossRef](#)] [[PubMed](#)]
61. Magri, D.C. Recent Progress on the Evolution of Pourbaix Sensors: Molecular Logic Gates for Protons and Oxidants. *Chemosensors* **2018**, *6*, 48. [[CrossRef](#)]
62. Magri, D.C. Logical sensing with fluorescent molecular logic gates based on photoinduced electron transfer. *Coord. Chem. Rev.* **2021**, *426*, 213598. [[CrossRef](#)]
63. Bozdemir, O.A.; Guliyev, R.; Buyukcakir, O.; Selcuk, S.; Kolemen, S.; Gulseren, G.; Nalbantoglu, T.; Boyaci, H.; Akkaya, E.U. Selective Manipulation of ICT and PET Processes in Styryl-Bodipy Derivatives: Applications in Molecular Logic and Fluorescence Sensing of Metal Ions. *J. Am. Chem. Soc.* **2010**, *132*, 8029. [[CrossRef](#)] [[PubMed](#)]
64. Tzeli, D.; Petsalakis, I.D.; Theodorakopoulos, G. Theoretical study of the photophysical processes of a styryl-bodipy derivative eliciting an AND molecular logic gate response. *Int. J. Quantum Chem.* **2019**, *119*, e25958. [[CrossRef](#)]

65. Tzeli, D.; Petsalakis, I.D.; Theodorakopoulos, G. The solvent effect on a styryl-bodipy derivative functioning as an AND molecular logic gate *Int. J. Quantum Chem.* **2020**, *120*, e26181. [[CrossRef](#)]
66. Velmurugan, K.; Vickram, R.; Jipsa, C.V.; Karthick, R.; Prabakaran, G.; Suresh, S.; Prabhu, J.; Velraj, G.; Tang, L.; Nandhakumar, R. Quinoline based reversible fluorescent probe for Pb²⁺; applications in milk, bioimaging and INHIBIT molecular logic gate. *Food Chem.* **2021**, *348*, 129098. [[CrossRef](#)] [[PubMed](#)]
67. Bahta, M.; Ahmed, N. A novel 1,8-naphthalimide as highly selective naked-eye and ratiometric fluorescent sensor for detection of Hg²⁺ ions. *J. Photochem. Photobiol. A Chem.* **2019**, *373*, 154–161. [[CrossRef](#)]
68. Fu, Q.-Q.; Hu, J.-H.; Yao, Y.; Yin, Z.-Y.; Gui, K.; Xu, N.; Niu, L.-Y.; Zhang, Y.-Q. A benzimidazole derivative based LMCT sensor for the detection of Cu²⁺ in DMSO/H₂O (2:3 v/v) solution and its application in implication logic gates. *J. Photochem. Photobiol. A Chem.* **2020**, *391*, 112358. [[CrossRef](#)]
69. Mukherjee, S.; Betal, S. Sensing phenomena, extraction and recovery of Cu²⁺ followed by smart phone application using a luminescent pyrene based chemosensor. *J. Lumin.* **2018**, *204*, 145–153. [[CrossRef](#)]
70. Ray, A.; Bar, N.; Chowdhury, P.; Biswas, D.; Ghosh, K.; Mandi, A.; Das, G.K. Reevaluation of copper(II)-Schiff base complex for sensing of D-penicillamine and development of a molecular logic gate: A combined approach. *Polyhedron* **2023**, *243*, 116563. [[CrossRef](#)]
71. Ryu, H.; Park, J.; Kim, H.K.; Park, J.Y.; Kim, S.-T.; Baik, M.-H. Pitfalls in Computational Modeling of Chemical Reactions and how to Avoid Them. *Organometallics* **2018**, *37*, 3228–3239. [[CrossRef](#)]
72. Andrada, D.M.; Holzmann, N.; Hamadi, T.; Frenking, G. Direct estimate of the internal π -donation to the carbene centre within N-heterocyclic carbenes and related molecules. *Beilstein J. Org. Chem.* **2015**, *11*, 2727–2736. [[CrossRef](#)] [[PubMed](#)]
73. Munz, D. Pushing Electrons—Which Carbene Ligand for Which Application? *Organometallics* **2018**, *37*, 275–289. [[CrossRef](#)]
74. Maser, L.; Herritsch, J.; Langer, R. Carbodiphosphorane-based nickel pincer complexes and their (de)protonated analogues: Dimerisation, ligand tautomers and proton affinities. *Dalton Trans.* **2018**, *47*, 10544–10552. [[CrossRef](#)] [[PubMed](#)]
75. Klein, M.; Sundermeyer, J. Modular Design Strategy toward Second-Generation Tridentate Carbodiphosphorane N,C,N Ligands with a Central Four-Electron Carbon Donor Motif and Their Complexes. *Organometallics* **2021**, *40*, 2090–2099. [[CrossRef](#)]
76. Marcum, J.S.; Cervarich, T.N.; Manan, R.S.; Roberts, C.C.; Meek, S.J. (CDC)-Rhodium-Catalyzed Hydroallylation of Vinylarenes and 1,3-Dienes with AllylTrifluoroborates. *ACS Catal.* **2019**, *9*, 5881–5889. [[CrossRef](#)]
77. Tzeliou, C.E.; Mermigki, M.A.; Tzeli, D. Review on the QM/MM Methodologies and Their Application to Metalloproteins. *Molecules* **2022**, *27*, 2660. [[CrossRef](#)]
78. Ferentinos, E.; Tzeli, D.; Sottini, S.; Groenen, E.J.J.; Ozerov, M.; Poneti, G.; Kaniewska-Laskowska, K.; Krzystek, J.; Kyritsis, P. Magnetic anisotropy and structural flexibility in the field-induced single ion magnets [Co{(OPPh₂)(EPPH₂)N₂}]₂, E = S, Se, explored by experimental and computational methods. *Dalton Trans.* **2023**, *52*, 2036–2050. [[CrossRef](#)] [[PubMed](#)]
79. Shimoyama, Y.; Ishizuka, T.; Kotani, H.; Shiota, Y.; Yoshizawa, K.; Mieda, K.; Ogura, T.; Okajima, T.; Nozawa, S.; Kojima, T. A Ruthenium(III)-Oxyl Complex Bearing Strong Radical Character. *Angew. Chem. Int. Ed.* **2016**, *55*, 14041–14045. [[CrossRef](#)] [[PubMed](#)]
80. Tseng, H.-W.; Zong, R.; Muckerman, J.T.; Thummel, R. Mononuclear ruthenium(II) complexes that catalyze water oxidation. *Inorg. Chem.* **2008**, *47*, 11763–11773. [[CrossRef](#)] [[PubMed](#)]
81. Pushkar, Y.; Moonshiram, D.; Purohit, V.; Yan, L.; Alperovich, I. Spectroscopic Analysis of Catalytic Water Oxidation by [Ru^{II}(bpy)(tpy)H₂O]²⁺ Suggests That Ru^V=O Is Not a Rate-Limiting Intermediate. *J. Am. Chem. Soc.* **2014**, *136*, 11938–11945. [[CrossRef](#)] [[PubMed](#)]
82. Drosou, M.; Kamatsos, F.; Ioannidis, G.; Zarkadoulas, A.; Mitsopoulou, C.; Papatriantafyllopoulou, C.; Tzeli, D. Reactivity and mechanism of photo- and electrocatalytic hydrogen evolution by a diimine copper(I) complex. *Catalysts* **2020**, *10*, 1302. [[CrossRef](#)]
83. Lee, C.; Yang, W.; Parr, R.G. Development of the Colle-Salvetti correlation-energy formula into a functional of the electron density. *Phys. Rev. B Condens. Matter Mater. Phys.* **1988**, *37*, 785–789. [[CrossRef](#)] [[PubMed](#)]
84. Zhao, Y.; Truhlar, D.G. The M06 suite of density functionals for main group thermochemistry, thermochemical kinetics, noncovalent interactions, excited states, and transition elements: Two new functionals and systematic testing of four M06-class functionals and 12 other functionals. *Theor. Chem. Acc.* **2008**, *120*, 215–241.
85. Steinmetz, M.; Grimme, S. Benchmark study of the performance of density functional theory for bond activations with (ni,pd)-based transition-metal catalysts. *ChemistryOpen* **2013**, *2*, 115–124. [[CrossRef](#)] [[PubMed](#)]
86. Rassolov, V.A.; Ratner, M.A.; Pople, J.A.; Redfern, P.C.; Curtiss, L.A. 6-31G* Basis Set for Third-Row Atoms. *J. Comp. Chem.* **2001**, *22*, 976–984. [[CrossRef](#)]
87. Hay, P.J.; Wadt, W.R. Ab initio effective core potentials for molecular calculations—Potentials for K to Au including the outermost core orbitals. *J. Chem. Phys.* **1985**, *82*, 299–310. [[CrossRef](#)]
88. Weigend, F.; Ahlrichs, R. Balanced basis sets of split valence, triple zeta valence and quadruple zeta valence quality for H to Rn: Design and assessment of accuracy. *Phys. Chem. Chem. Phys.* **2005**, *7*, 3297–3305. [[CrossRef](#)] [[PubMed](#)]
89. Kendall, R.A.; Dunning, T.H., Jr.; Harrison, R.J. Electron affinities of the first-row atoms revisited. Systematic basis sets and wave functions. *J. Chem. Phys.* **1992**, *96*, 6796–6806. [[CrossRef](#)]
90. Peterson, K.A.; Figgen, D.; Dolg, M.; Stoll, H. Energy-consistent relativistic pseudopotentials and correlation consistent basis sets for the 4d elements Y-Pd. *J. Chem. Phys.* **2007**, *126*, 124101. [[CrossRef](#)] [[PubMed](#)]

91. Miertuš, S.; Scrocco, E.; Tomasi, J. Electrostatic interaction of a solute with a continuum. A direct utilization of AB initio molecular potentials for the prevision of solvent effects. *Chem. Phys.* **1981**, *55*, 117–129. [[CrossRef](#)]
92. Caricato, M.; Mennucci, B.; Tomasi, J.; Ingrosso, F.; Cammi, R.; Corni, S.; Scalmani, G. Formation and relaxation of excited states in solution: A new time dependent polarizable continuum model based on time dependent density functional theory. *J. Chem. Phys.* **2006**, *124*, 124520. [[CrossRef](#)] [[PubMed](#)]
93. Malmqvist, P.-Å.; Roos, B.O. The CASSCF state interaction method. *Chem. Phys. Lett.* **1989**, *155*, 189–194. [[CrossRef](#)]
94. Angeli, C.; Cimraglia, R.; Evangelisti, S.; Leininger, T.; Malrieu, J.-P. Introduction of n-electron valence states for multireference perturbation theory. *J. Chem. Phys.* **2001**, *114*, 10252–10264. [[CrossRef](#)]
95. Bickelhaupt, F.; Hommes, N.; Guerra, C.; Baerends, E. The Carbon–Lithium Electron Pair Bond in $(\text{CH}_3\text{Li})_n$ ($n = 1, 2, 4$). *Organometallics* **1996**, *15*, 2923–2931. [[CrossRef](#)]
96. Ishikawa, S.; Madjarova, G.; Yamabe, T.J. First-Principles Study of the Lithium Interaction with Polycyclic Aromatic Hydrocarbons. *Phys. Chem. B* **2001**, *105*, 11986–11993. [[CrossRef](#)]
97. Maseras, F.; Morokuma, K. Application of the natural population analysis to transition-metal complexes. Should the empty metal p orbitals be included in the valence space? *Chem. Phys. Lett.* **1992**, *195*, 500–504. [[CrossRef](#)]
98. Guerra, C.F.; Handgraaf, J.-W.; Baerends, E.J.; Bickelhaupt, F.M. Voronoi deformation density (VDD) charges: Assessment of the Mulliken, Bader, Hirshfeld, Weinhold, and VDD methods for charge analysis. *J. Comput. Chem.* **2004**, *25*, 189–210. [[CrossRef](#)] [[PubMed](#)]
99. Marenich, A.V.; Jerome, S.V.; Cramer, C.J.; Truhlar, D.G. Charge Model 5: An Extension of Hirshfeld Population Analysis for the Accurate Description of Molecular Interactions in Gaseous and Condensed Phases. *J. Chem. Theory Comput.* **2012**, *8*, 527–541. [[CrossRef](#)] [[PubMed](#)]
100. Orbach, R.; Willner, B.; Willner, I. Catalytic nucleic acids (DNAzymes) as functional units for logic gates and computing circuits: From basic principles to practical applications. *Chem. Commun.* **2015**, *51*, 4144–4160. [[CrossRef](#)] [[PubMed](#)]
101. Ling, J.; Daly, B.; Silvester, V.A.; De Silva, A.P. Taking baby steps in molecular logic-based computation. *Chem. Commun.* **2015**, *40*, 8403–8409. [[CrossRef](#)] [[PubMed](#)]
102. Katz, E.; Minko, S. Enzyme-based logic systems interfaced with signal-responsive materials and electrodes. *Chem. Commun.* **2015**, *51*, 3493–3500. [[CrossRef](#)] [[PubMed](#)]
103. Andreasson, J.; Pischel, U. Molecules for security measures: From keypad locks to advanced communication protocols. *Chem. Soc. Rev.* **2018**, *47*, 2266–2279. [[CrossRef](#)] [[PubMed](#)]
104. Tzeli, D.; Petsalakis, I.D. Physical insights into molecular sensors, molecular logic gates, and photosensitizers in photodynamic therapy. *J. Chem.* **2019**, *2019*, 6793490. [[CrossRef](#)]
105. Yao, C.Y.; Lin, H.Y.; Crory, H.S.; de Silva, A.P. Supra-molecular agents running tasks intelligently (SMARTI): Recent developments in molecular logic-based computation. *Mol. Sys. Des. Eng.* **2020**, *5*, 1325–1353. [[CrossRef](#)]
106. Tzeli, D. Molecular logic gates. *J. Chem. Tech. App.* **2023**, *6*, 136.
107. Liu, L.; Liu, P.; Ga, L.; Ai, J. Advances in applications of molecular logic gates. *ACS Omega* **2021**, *6*, 30189–30204. [[CrossRef](#)] [[PubMed](#)]
108. Schneider, H.J. (Ed.) *Supramolecular Systems in Biomedical Fields*; Royal Society Chemistry: London, UK, 2013.
109. Ozlem, S.; Akkaya, E.U. Thinking outside the silicon box: Molecular and logic as an additional layer of selectivity in singlet oxygen generation for photodynamic therapy. *J. Am. Chem. Soc.* **2009**, *131*, 48–49. [[CrossRef](#)] [[PubMed](#)]
110. de Silva, A.P.; James, M.R.; McKinney, B.O.F.; Pears, D.A.; Weir, S.M. Molecular computational elements encode large populations of small objects. *Nat. Mater.* **2006**, *5*, 787–789. [[CrossRef](#)] [[PubMed](#)]
111. Torriero, A.A.J.; Mruthunjaya, A.K.V. Ferrocene-Based Electrochemical Sensors for Cations. *Inorganics* **2023**, *11*, 472. [[CrossRef](#)]
112. Fabbrizzi, L. The ferrocenium/ferrocene couple: A versatile redox switch. *ChemTexts* **2020**, *6*, 22. [[CrossRef](#)]

Disclaimer/Publisher’s Note: The statements, opinions and data contained in all publications are solely those of the individual author(s) and contributor(s) and not of MDPI and/or the editor(s). MDPI and/or the editor(s) disclaim responsibility for any injury to people or property resulting from any ideas, methods, instructions or products referred to in the content.